Vehicles Dynamics, Planning and Control of Robotic Cars

Final Report

Basem Shaker <basem.shaker@studenti.unitn.it>

Presented to: Gastone Pietro Rosati Papini

June 2022

Contents

Assignment 1

Tire Model Exercises - 1

1.1 Exercise 1 – Pure Longitudinal Slip

Q. Using the Pacejka Magic Formula, plot the longitudinal tire force F_{x0} obtained in pure longitudinal slip conditions, as a function of slip $\kappa \in$ [-1, 1]. Which comments are you able to make about the obtained graph?

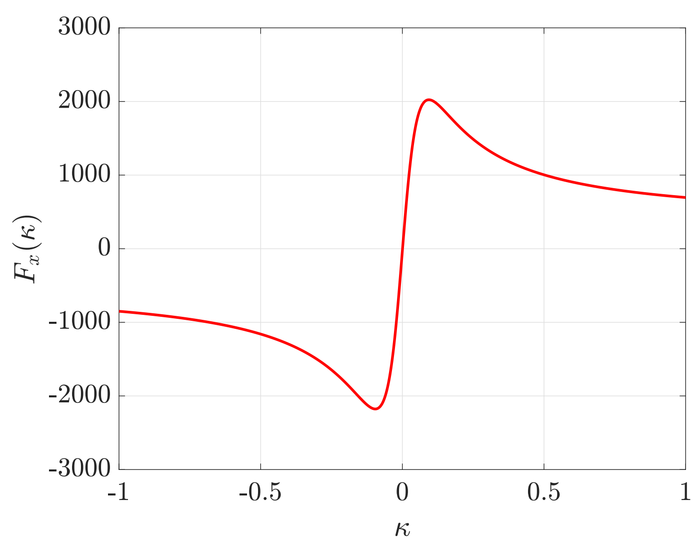

Figure 1.1: F_{x0} as a function of slip

When κ (longitudinal slip) increases, F_x grows until it reaches a saturation limit. Furthermore, the slip zone grows, and the adherence area decreases. That means, the total tire force F_x keeps growing until it reaches a peak and a saturation limit as shown in the graph below.

κ (longitudinal slip) is positive when the tire is accelerating, negative during braking, and reaches -1 when the wheel locks.

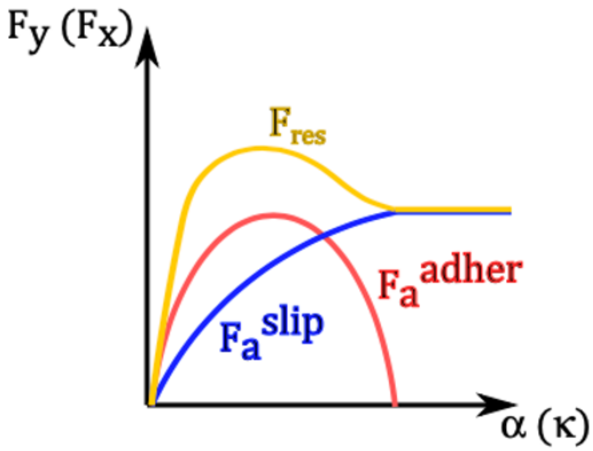

Figure 1.2: Slip and adherence forces

Q. If you were supposed to design a traction control system for maximizing vehicle longitudinal acceleration, which would be the target value of longitudinal slip κ that you would try to achieve?

Acceleration is directly proportional to the force [F=ma] if the mass is constant. If I want to maximize the vehicle longitudinal acceleration, I would need to maximize the longitudinal force [F_x]. F_x is highest at the saturation limit, which in this example happens at slip κ = 0.094, and yields an F_x of 2022.99 N.

Q. Assuming that wheel rotational speed is ω = 70 rad/s, tire effective rolling radius is R_e = 0.2 m, while the longitudinal component of tire contact point speed υ_{Cx} = 13 m/s, compute the longitudinal slip κ. In these conditions, is the wheel accelerating, braking or is it in pure rolling? Compute also the corresponding longitudinal tire force F_{x0}

Using Matlab, the calculated longitudinal slip κ = 0.0769 and the calculated longitudinal force F_x is = 1990.65 N. the longitudinal slip is positive (>0), which means that the wheel is accelerating.

Q. Compute the cornering stiffness Cfκ, that is the derivative for κ = 0 of the F_{x0}. Up to which value of κ is the linear approximation of Pacejka curve acceptable?

The cornering Stiffness Cfκ is equal to the derivative of the longitudinal force with respect to the longitudinal slip when the longitudinal slip is equal to zero. This means its equal to the slope at the origin (x=y=0) or equal to BCD function as shown in Figure 1.3. The calculated cornering stiffness is Cfκ = 47909.4

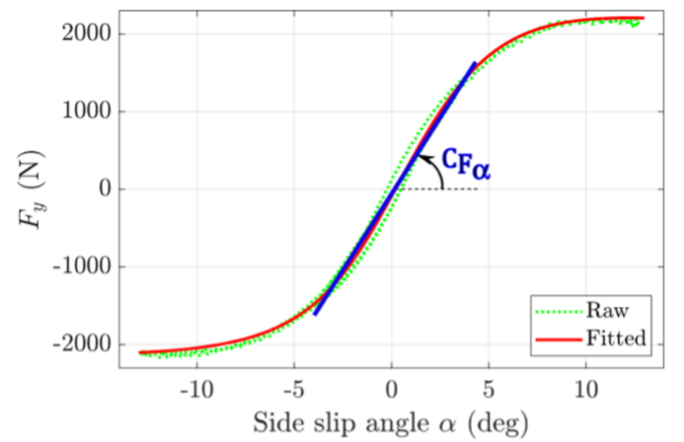

Figure 1.3: cornering stiffness as a linear approximation

The linear approximation allows to neglect the complex Pacejka Magic Formula, but it is valid only for small κ. At $\kappa = 0.02$, the percent difference is already at 10% as shown in Figure 1.4.

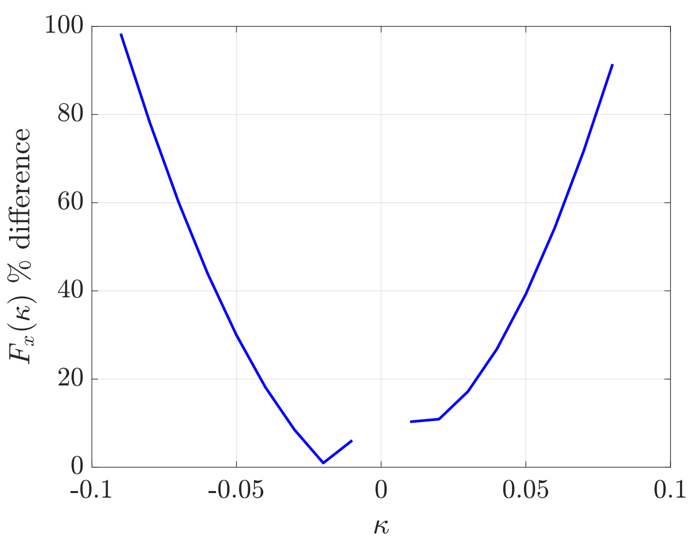

Figure 1.4: % difference in κ using linear approximation vs Pacejka formula

1.2 Exercise 2 - Combined Slip

Q. Assume that the tire contact point velocity components along the tire x and y axes are υ_{Cx} = 15 m/s and υ_{Cy} = -1.3 m/s, respectively. Calculate the side slip angle α. Moreover, compute the combined tire force F_x using this value of α, for a longitudinal slip κ = 0.08.

Alpha can be calculated using the practical slip approach:

$$\text{side slip angle } \alpha = -\arctan(\frac{\upsilon_{sy}}{\upsilon_{Cx}}) = -\arctan(\frac{\upsilon_{Cy}}{\upsilon_{Cx}}) \tag{1.1}$$

Using equation 1.2 to calculate G_{xa} (weighing function). Once calculated, F_{x0} can now be multiplied by G_{xa} (weighing function) to get the combined tire force F_x.

$$G_{xa} = -D_{xa}\cos(C_{xa}\arctan(B_{xa}(\alpha + S_{Hxa})) \tag{1.2}$$

$$F_{x0} = D_x \sin(C_x \arctan(B_x\kappa_x - E_x(B_x\kappa_x - \arctan(B_x\kappa_x))) \tag{1.3}$$

$$F_x = G_{xa}F_{x0} \tag{1.4}$$

Using Matlab to calculate the side slip angle α and combined tire force:

calculated side slip alpha = 0.086451
calculated weighing function = 0.724417
calculated combined force F_x = 1450.424623

Q. Plot the combined longitudinal tire force F_x as a function of $\kappa \in$ [-1, 1], for the following levels of side slip angle α = {0, 2, 4, 6, 8} degrees. Which comments can you make about the 5 curves obtained in this way? Finally, plot the weighting function G_{xa} as a function of $\kappa \in$ [-1, 1] for each of the previously defined values of α, and briefly comment also these 5 curves.

Figure 1.5 shows plots obtained for the combined longitudinal force F_x for each side slip angle as a function of the longitudinal slip κ. The maximum combined longitudinal force F_x keeps decreasing with higher side slip α.

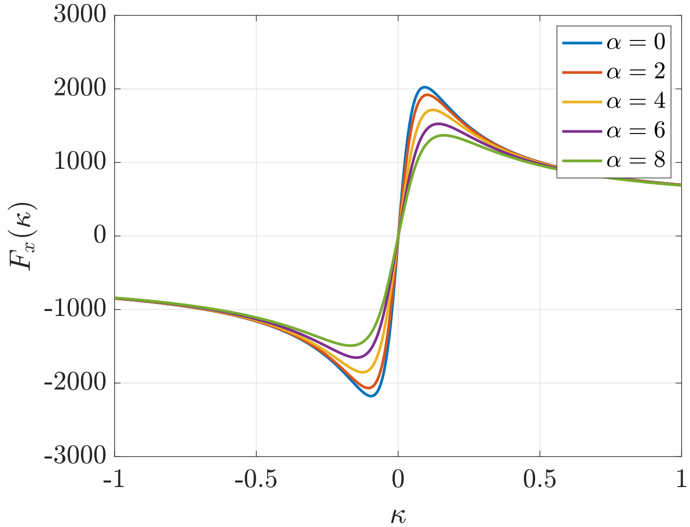

Figure 1.5: combined longitudinal force F_x as a function of κ

Figure 1.6 shows the plots obtained for the weighing function G_{xa} for each side slip angle as a function of the longitudinal slip κ. Higher side slip α decreases the weighing function, which in effect decreases the combined longitudinal force F_x. The effect of the weighing function is quite more potent around $\kappa = 0$, and that effect decreases the further away we are from it.

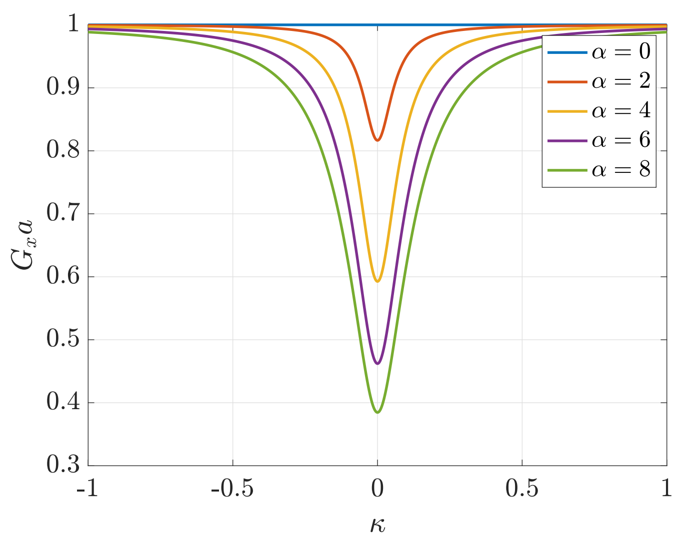

Figure 1.6: Weighing function G_{xa} as a function of κ

Assignment 2

Tire Model Exercises - 2

2.1 Exercise 1 – Understanding Tire Data

Q. Plot the raw data in different graphs, specifically focusing on κ, α, γ, F_z and pressure P. Comment on what you see. What is, according to you, the main target of these tests?

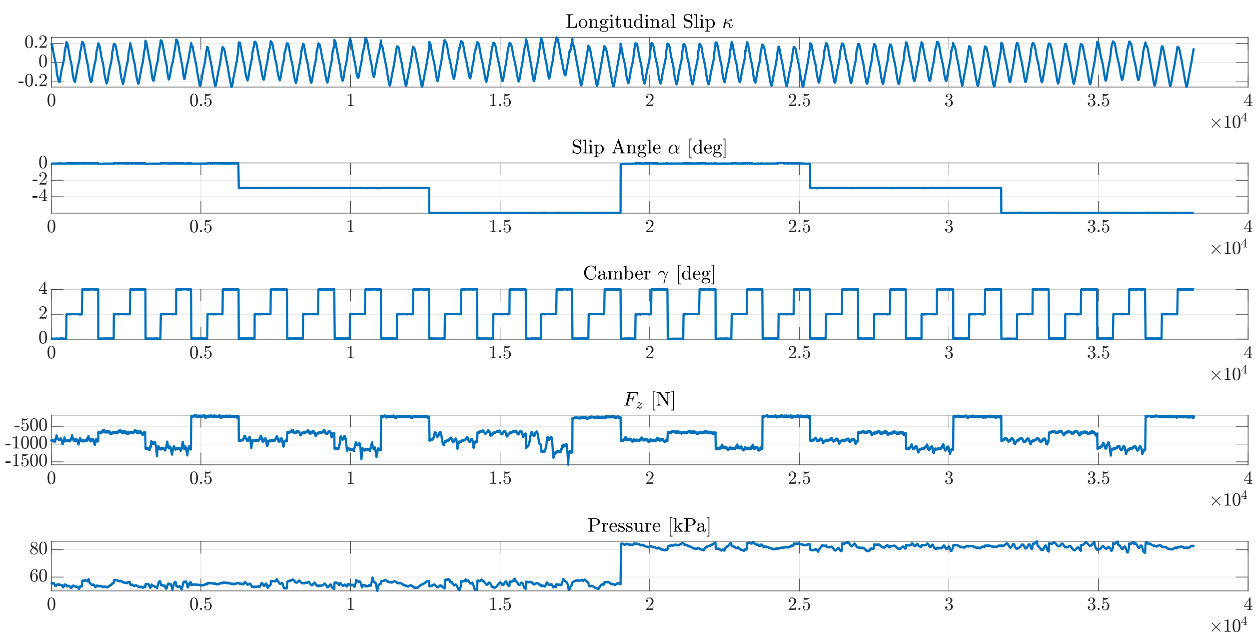

Figure 2.1: raw data

From the five plotted variables in Figure 2.1, it appears that the longitudinal slip, slip angle, camber, vertical force, and pressure are all showing repeat patterns. That means that those five variables are controlled to measure and test their effect on the longitudinal force F_x. Note that the longitudinal slip κ for each test spanned from 0.2 to -0.2 and then back again to 0.2. The data extracted for the following questions only took the first half of each separate test. Furthermore, only data that had P = 83 kPa were used, because the data seemed noisier with P = 55 kPa, especially with F_z data.

Q. Focus on the data with α =0 and γ =0, and plot the curves F_x vs κ for each of the 4 vertical loads F_z used in the experiments. Plot the 4 curves on the same graph, with different colors. Comment on what you see.

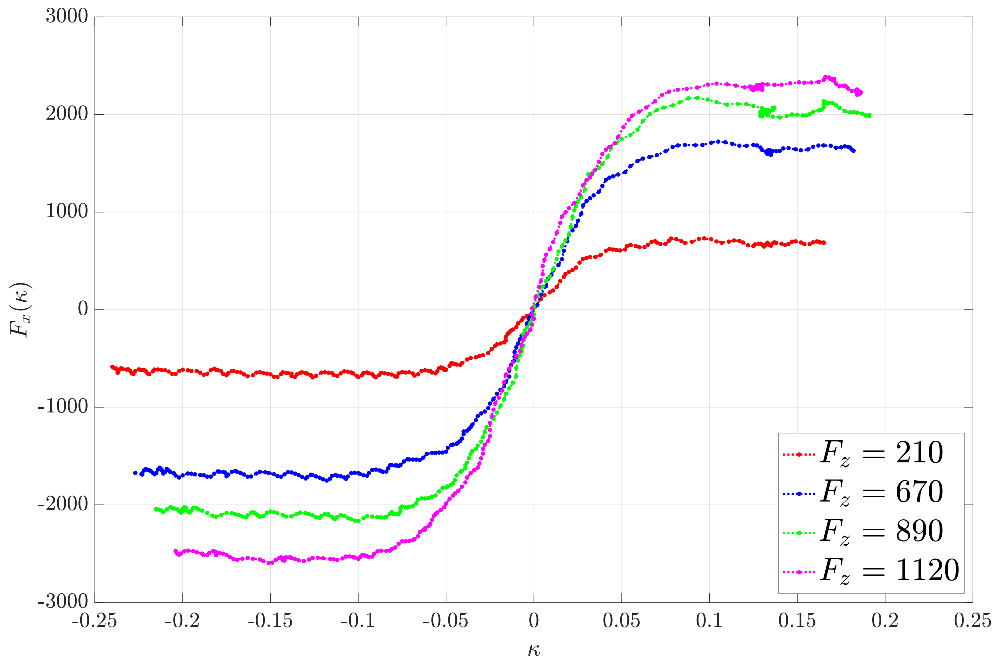

Figure 2.2: κ vs F_x based on vertical force

Figure 2.2 suggests that the Longitudinal Force F_x increases with the vertical force F_z. There is some dependency on the vertical force. If you double the vertical force, it does not mean the longitudinal force will double. In some parts there is a linear dependency, but in others it is not the case.

Q. Focus on the data with γ =0 and F_z = 150 lbf ≈ 670N, and plot the curves F_x vs κ for each of the 3 side slip angles α used in the experiments. Plot the 3 curves on the same graph, with different colors. Comment on what you see.

The Longitudinal Force F_x in Figure 2.3 shows an inverse relationship with the side slip angle.

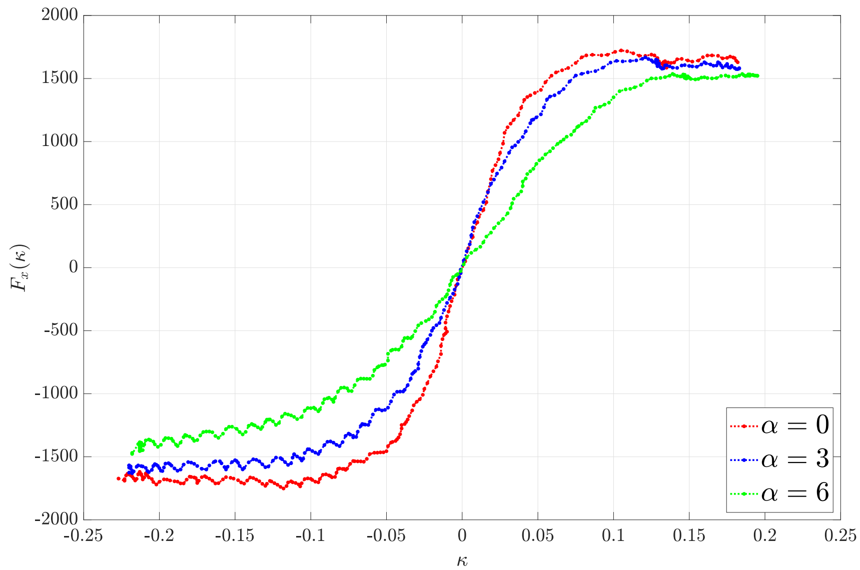

Figure 2.3: κ vs F_x at vertical force = 670 based on slip angle

2.2 Exercise 2 - Fitting Tire Data

Q. First consider the data with $F_z = F_{z0}$ =890N, γ =0 and α =0, and fit the coefficients X1 = $\{p_{Cx1}, p_{dx1}, p_{Ex1}, p_{Ex4}, p_{Kx1}, p_{Hx1}, p_{Vx1}\}$. Plot the fitted curve F_x vs κ that you obtained in these nominal conditions, together with the raw data.

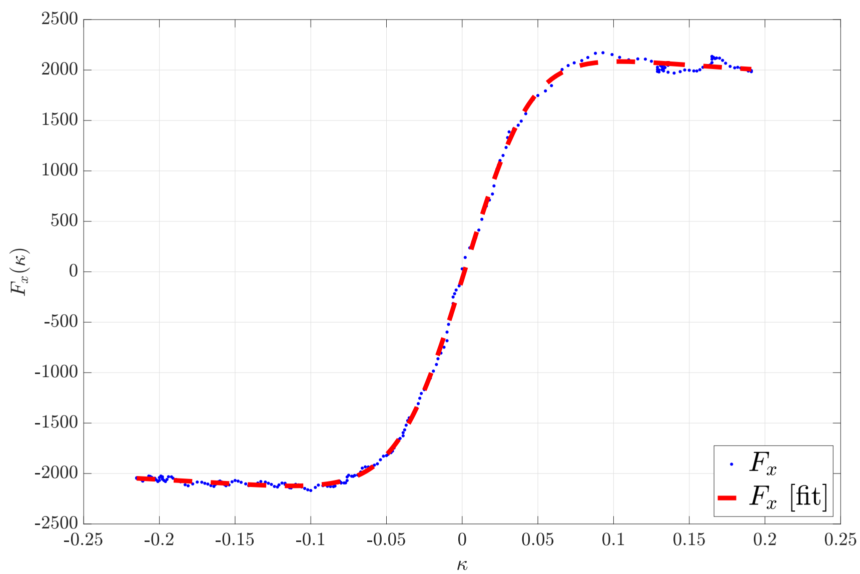

Figure 2.4: Fitted F_{x0} after optimizing first 7 parameters compared to test data vs κ

In Figure 2.4, the data was filtered based on the following criteria: $F_{z0} = 890$, $\alpha = 0$, $\gamma = 0$. The first 7 coefficients were optimized using the $fmincon$ function in Matlab. I started with a random coefficients initial guess vector. The initial guess vector has proven to be quite important as running the code multiple times showed a curve that did not fit the data at all, which means the optimizer was stuck at a local minima. However, most of the time the initial guess gave a very good fit that converged to the correct global minima. Later on I optimized the initial guesses to give consistent good fitting results based on trial and error.

Q. Consider data with the 4 different values of F_z, but still $\gamma = 0$ (and $\alpha = 0$). This enables the fitting of the parameters: X2 =$\{p_{dx2}, p_{Ex2}, p_{Ex3}, p_{Hx2}, p_{Kx2}, p_{Kx3}, p_{Vx2}\}$. Plot fitted and raw curves F_{x0} vs κ for the 4 values of F_z and comment the results.

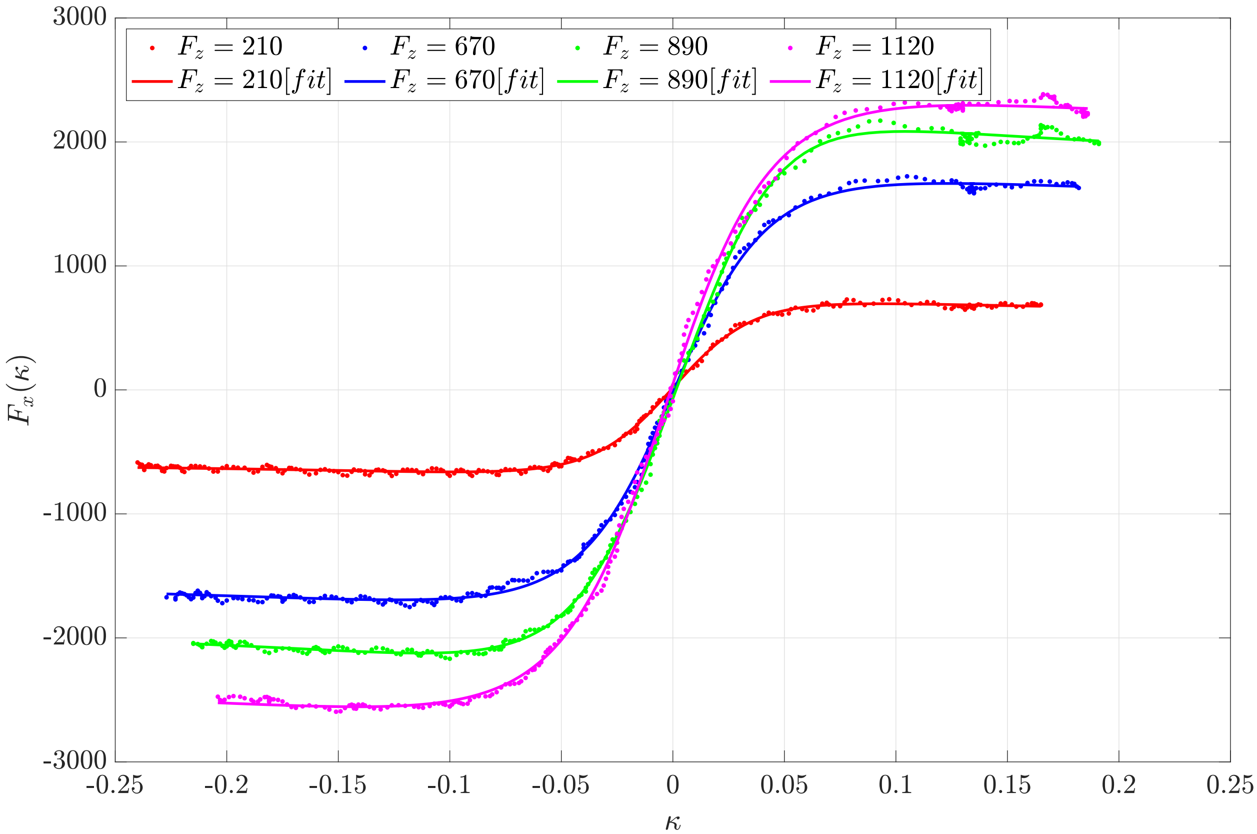

Figure 2.5: Fitted F_x vs test data after second fitting for each F_z

The real F_x data for each separate F_z are plotted against the output of the second fitting in Figure 2.5. The fitted data appear to match the test data quite well. This means the fitting results are adequate to approximate the longitudinal force F_x for vertical forces F_z that are different from the originally tested one.

Q. Now consider the data with the 3 different values of γ, but with $F_z = F_{z0}$ (and $\alpha = 0$). Plot the fitted and raw curves F_{x0} vs κ for the 3 values of γ and comment the results.

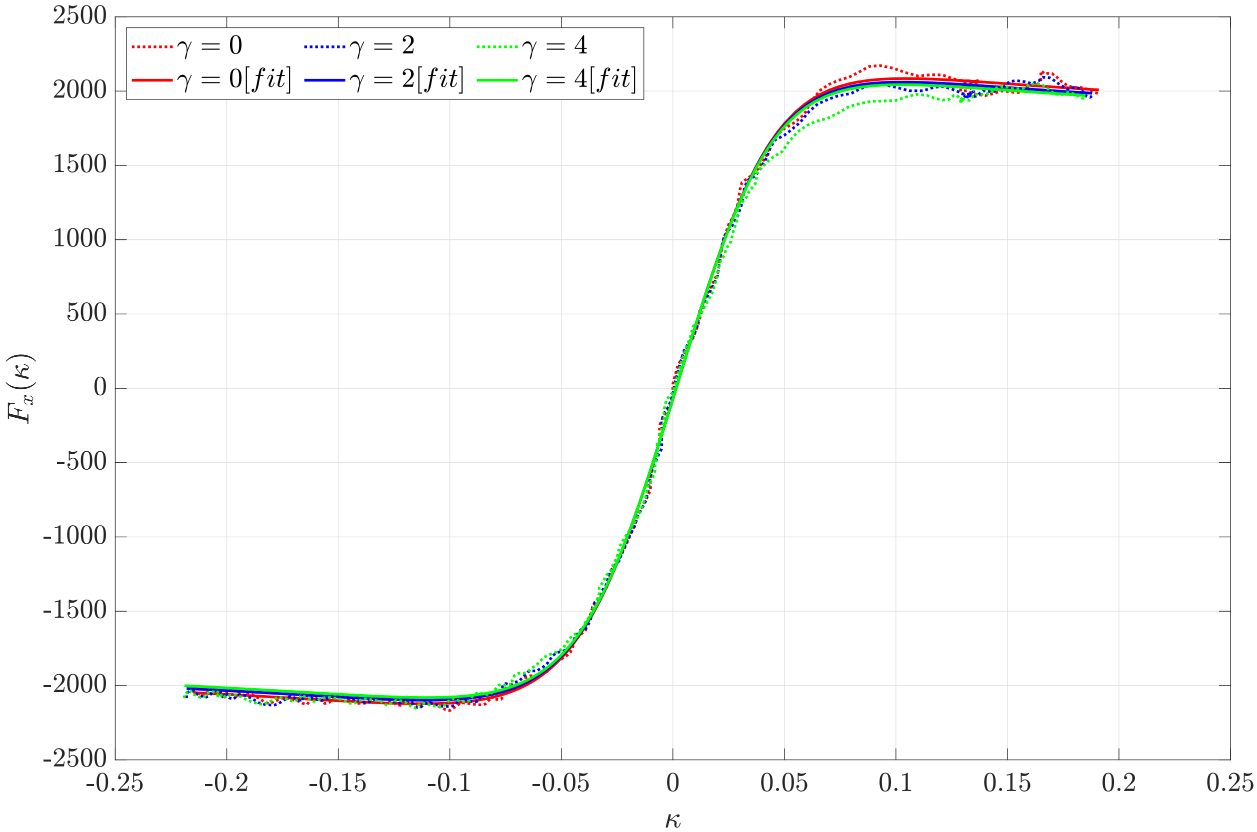

Figure 2.6: Fitted F_x vs test data after third fitting for each γ

Figure 2.6 shows the results of the third fitting. The data from $\gamma = 0$ fits properly as shown previously in Figure 2.4. However, the fitting on the other γ values did not match completely. Trying different initial values for p_{dx2} did not yield any better results.

Assignment 3

Vehicle Data Analysis Exercises

3.1 Exercise 1 – Understanding Vehicle Data

Q. Plot lateral and longitudinal velocity

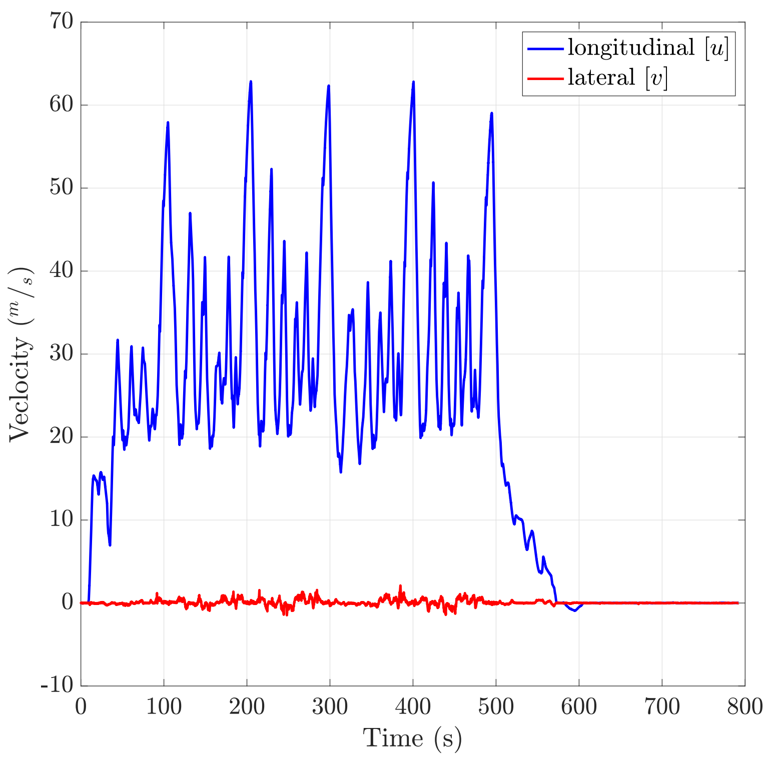

Figure 3.1: lateral and longitudinal velocity vs time

From Figure 3.1, the magnitude of the longitudinal velocity u is higher than the lateral velocity v. This matches what was expected as the vehicle mainly moves longitudinally and only laterally while slipping. v also appears to have larger variations.

Q. Evaluate the longitudinal speed using the Hall-effect wheel speed sensors and compare the data with the INS data

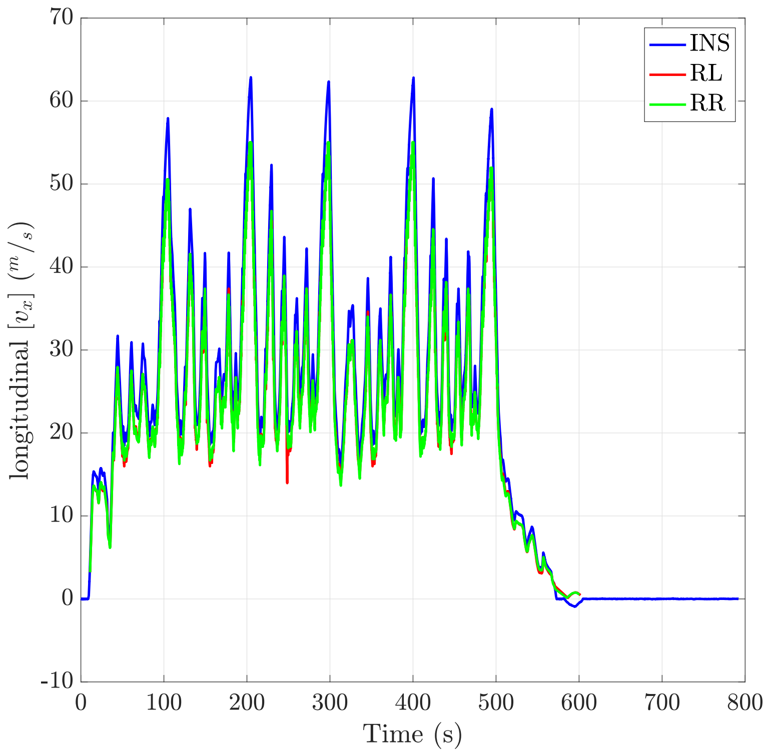

Figure 3.2: INS vs RL/RR hall effect sensors v_x

The longitudinal speed for the vehicle was calculated using the hall effect sensor data. Only the rear wheels [left and right] were used for the calculation. That is because they do not have a torque applied on them and they are "free rolling". Every change in voltage [tick] means a full revolution of the tire. The time difference between 2 ticks was calculated [$\overline{T}$] and used in equation 3.1 to estimate the longitudinal speed [Where c is the wheel circumference]:

$$v_{wheel} = \frac{c}{\overline{T}} \tag{3.1}$$

The INS velocity is sometimes bigger than the hall effect calculated speeds, especially during braking [partial wheel lock]. There is no obvious difference between them during acceleration, which mean no significant wheel spin has been detected (Figure 3.2).

Q. Evaluate the lateral acceleration using the relation with the Ω and u.

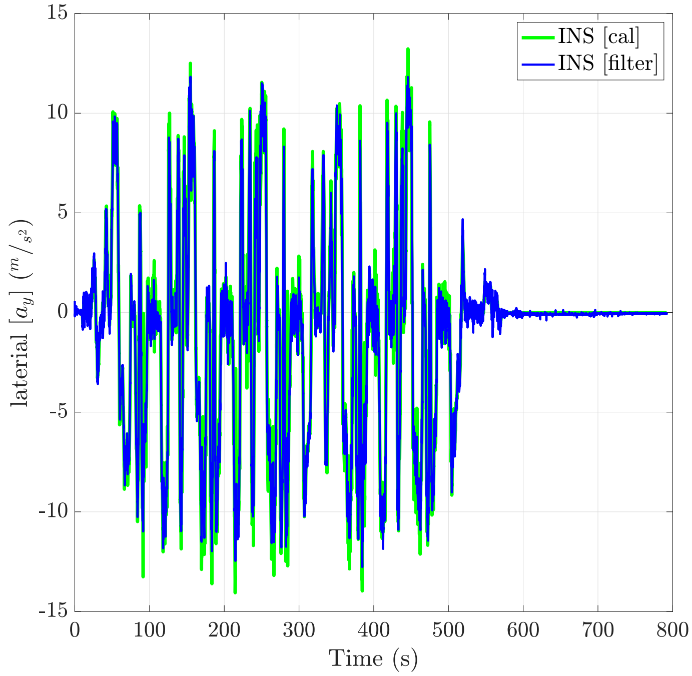

Figure 3.3: filtered INS vs calculated a_y

The lateral acceleration was calculated by multiplying the yaw rate by the longitudinal velocity, and is shown in Figure 3.3. This means that the following assumptions were true:

1. The vehicle has stayed in steady state where $\dot{v}$ is small and $a_y \simeq \Omega u$
2. the road banking was negligible

Q. Comparing the longitudinal acceleration measured by INS with the one obtained by derivation of the longitudinal speed measured from the Hall sensors.

The derived acceleration a_x [shown in Figure 3.4] is quite noisier than the one provided by INS. The derived acceleration was filtered using a moving mean. This resulted in a far better matching acceleration compared to the INS data.

Q. Evaluate the side slip angle.

In Figure 3.5, the side slip angle β was calculated using the equation $\beta = \arctan(v/u)$. It appears that both the calculated and the INS provided β are similar, meaning that the INS is using the same formula. When $u \simeq 0$ the calculation becomes very noisy. The INS might be employing sensor fusion to suppress that noise. $\beta \in [-3, 5]$ which is considered small.

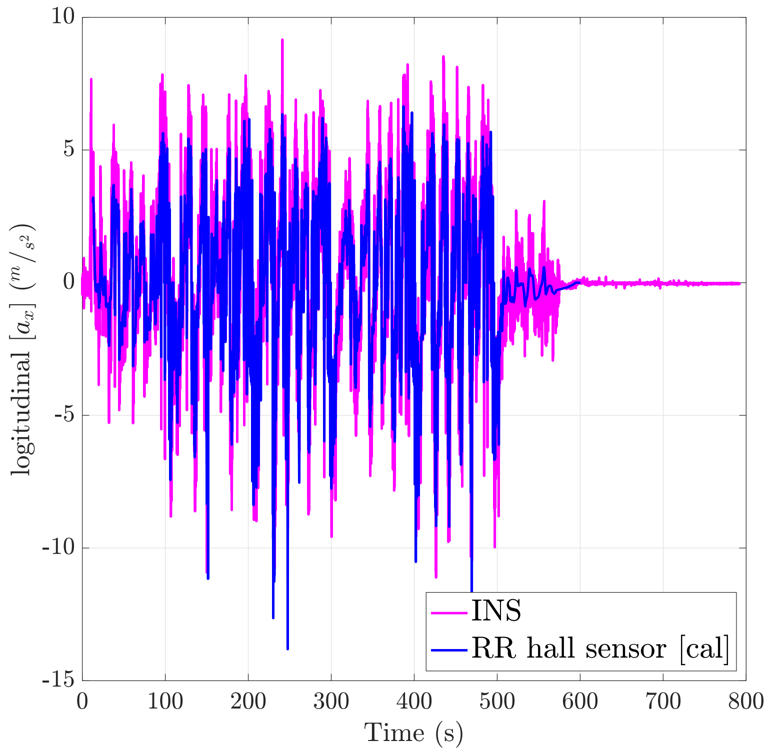

Figure 3.4: INS vs RR wheel hall effect derived a_x

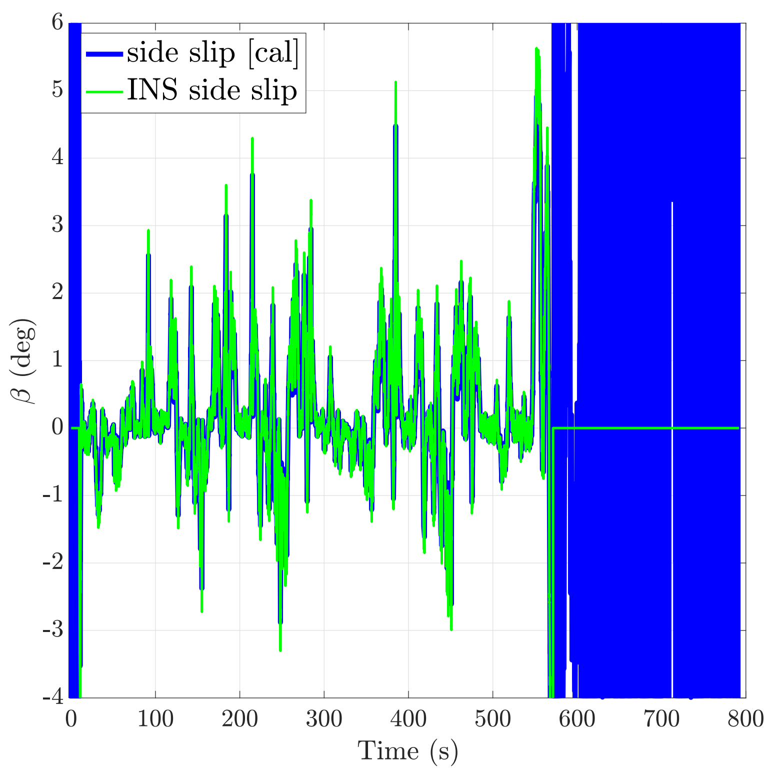

Figure 3.5: INS vs calculated side slip angle

Assignment 4

Vehicle Model Exercises

4.1 Exercise 1 - Vehicle Model Implementation

Q. For each maneuver, plot and comment the main results that you obtain, particularly focusing on tire forces and moments ($\{F_x, F_y, F_z, M_z\}$) and tire slips ($\{\kappa, \alpha\}$).

1. initial conditions: $u_0 = 30$ km/h
   simulation timing: $T_s = 0.001$ s, $T_f = 20$ s
   requested pedal: req_pedal = 1
   requested steering wheel angle: req_steer = 0 deg.

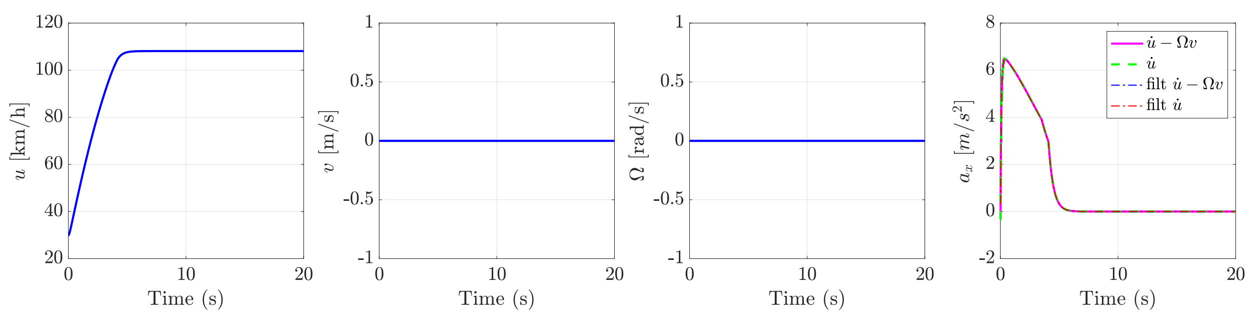

Figure 4.1: vehicle motion graphs [maneuver #1]

Figure 4.1 shows the motion graphs of the first maneuver. The vehicle starts from 30 km/h, with no steering input and full throttle. The velocity increased until it reached full speed of 108 km/h within 5 seconds. All upcoming graphs are influenced by the acceleration profile.

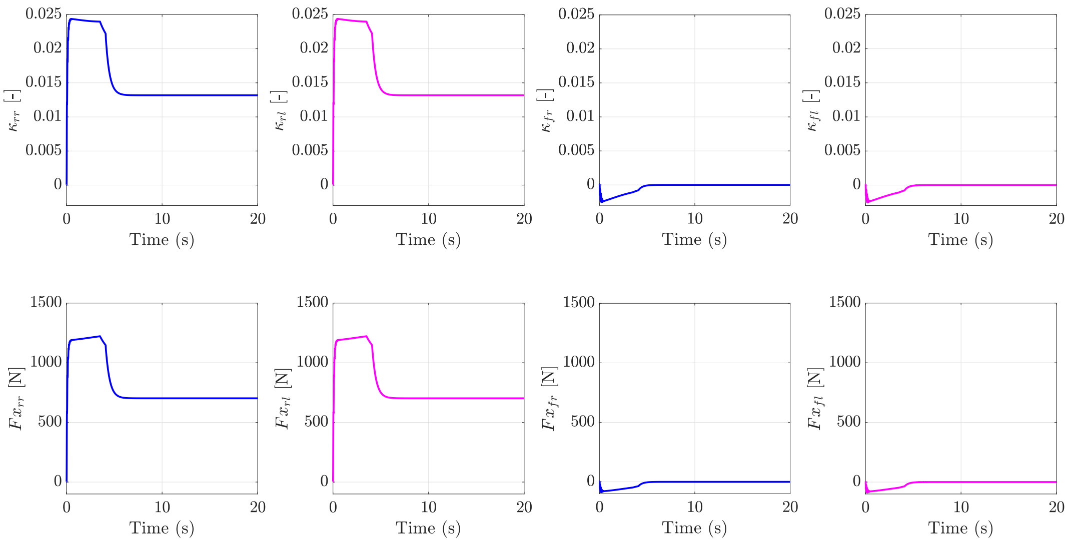

Figure 4.2: longitudinal slip κ and longitudinal forces F_x [maneuver #1]

The graphs in Figure 4.2 shows no difference between both right tires [and similarly the left tires] as the vehicle was moving straight without steering input. However, both rear tires show much higher κ and F_y. This was expected as the vehicle is rear-wheel drive and torque applied from the motors would increase both the slip and force experienced by the rear tires.

During the vehicle's acceleration to maximum speed [between 0 and 5 seconds] all tires showed higher slip and force. Once maximum speed is reached [acceleration is zero], the slips and forces decrease across all tires. The front tires go to zero, while the rears do not, as the motors must still keep applying [decreased] torque to keep the vehicle at speed.

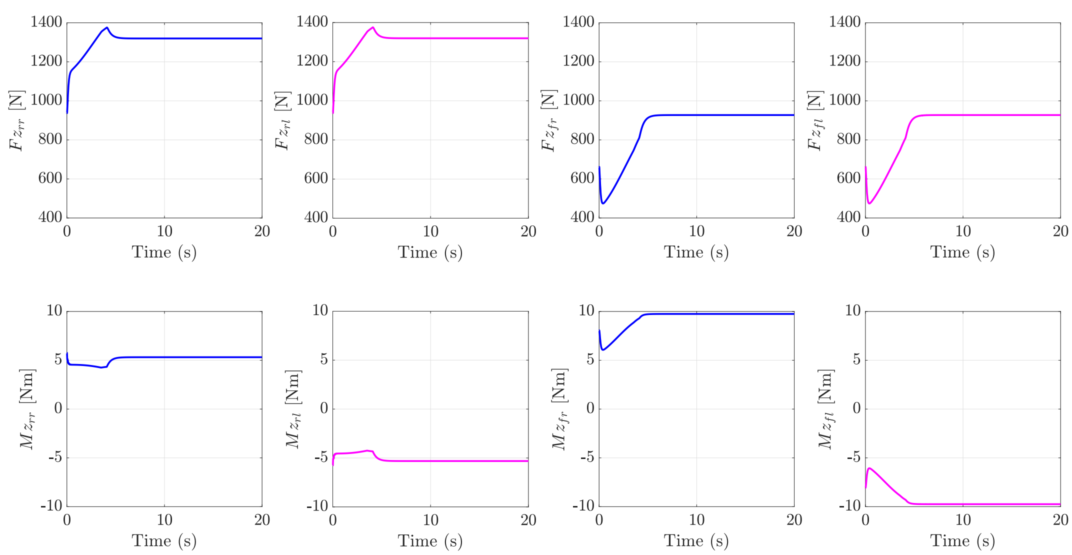

Figure 4.3: Vertical forces F_z and self aligning torque M_z [maneuver #1]

The aerodynamics load F_A increases as speed increases. As shown in Figure 4.3, the vertical force F_z increases across all tires because it relies on F_A. The vertical loads are calculated using Equation 4.1:

$$\begin{aligned} F_{zr} &= mg\frac{L_f}{L} + F_{Azr} + F_x\frac{h_G}{L} - \frac{I_{yz}}{L}\dot{\Omega} \\ F_{zf} &= mg\frac{L_r}{L} + F_{Azf} + F_x\frac{h_G}{L} - \frac{I_{yz}}{L}\dot{\Omega} \end{aligned} \tag{4.1}$$

They later reach steady state once the car stops accelerating. the rear tires show a peak in F_z due to the drop in acceleration a_y towards nearing maximum speed, which decreased the lateral load transfer on the rear tires.

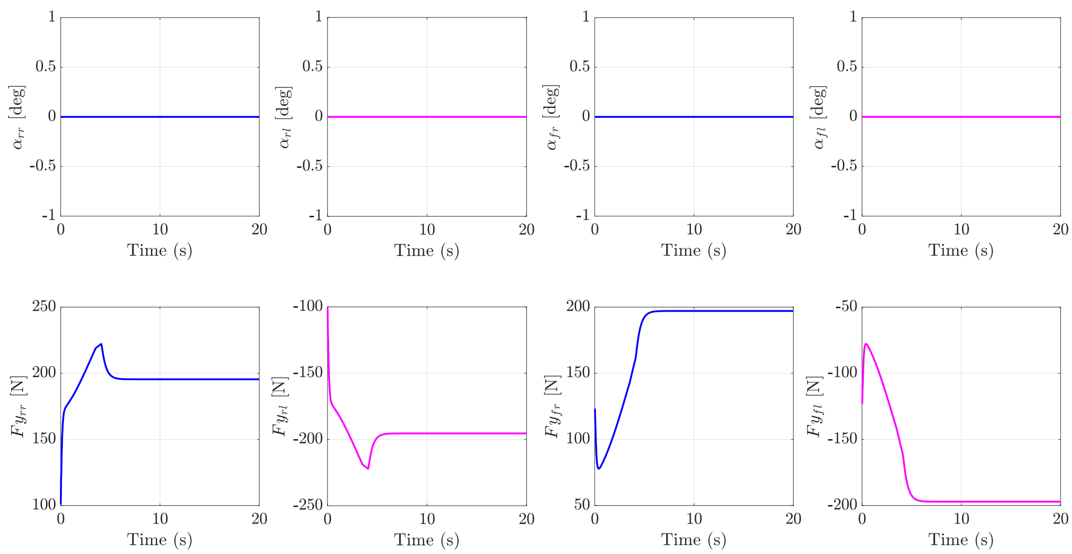

Figure 4.4: side slip angle α and lateral forces F_y [maneuver #1]

As previously mentioned, the vehicle has no steering input, which is why the side slip angle α for all tires are zero [Figure 4.4]. Furthermore, the magnitude of the lateral forces on the right tires are equal [and similarly the left tires]. The right tires' lateral forces are opposite in direction compared to the left tires and equal in magnitude, thus making them cancel out keeping the vehicle moving straight. F_y is smaller than F_x for all the tires. The self aligning torque M_z profiles previously shown in Figure 4.3 resemble the lateral forces profiles for each tire as they are trying to counter their effect on the steering.

During acceleration, the lateral forces F_y across all tires increase because the vertical forces F_z increased. The lateral forces relies on the vertical forces in the pacejka calculations, which is why both the F_y and F_z profiles match for front and rear tires.

2. initial conditions: u_0 = 100 km/h
   simulation timing: T_s = 0.001 s, T_f = 1.5 s
   requested pedal: req_pedal = -1
   requested steering wheel angle: req_steer = 0 deg.

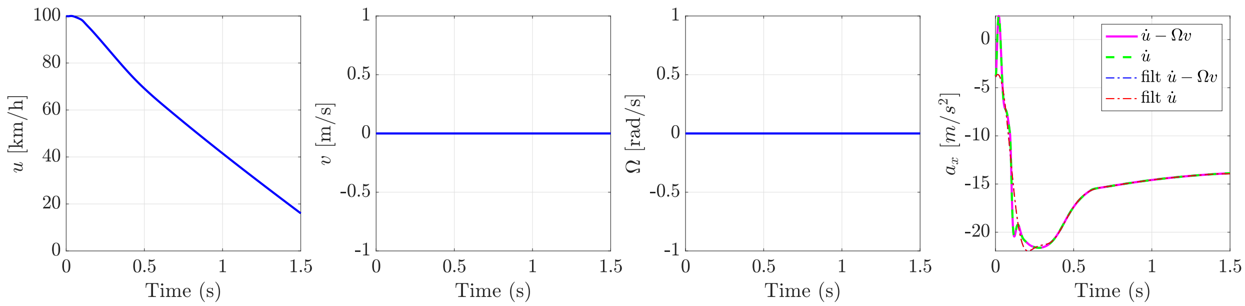

Figure 4.5: vehicle motion graphs [maneuver #2]

Figure 4.5 shows the motion graphs of the second maneuver. The vehicle starts from 100 km/h, with no steering input and applying full brakes. The velocity dropped to 16 km/h within the specified 1.5 seconds. The deceleration shows a decrease after 0.27 seconds as the rear tires start slipping and going into a full wheel lock as shown in Figure 4.6.

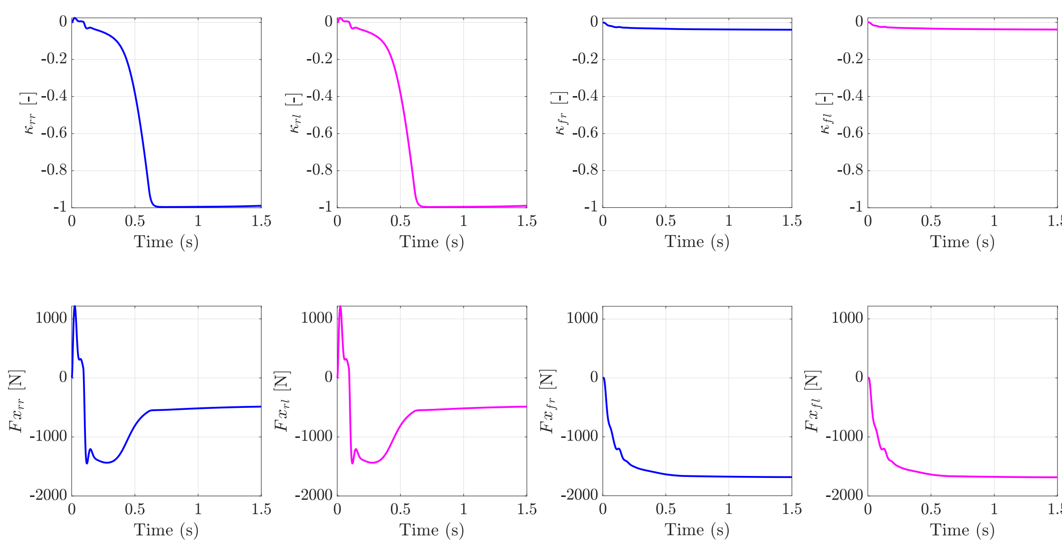

Figure 4.6: longitudinal slip κ and longitudinal forces F_x [maneuver #2]

This maneuver also doesn't have steering input, which is why the graphs in Figure 4.6 show no difference between both right and left tires. The longitudinal forces F_x for all tires increase in the opposite direction because the vehicle is decelerating. The longitudinal slip κ for the rear tires go to -1, which means both tires went into wheel lock. F_x decreases once wheel lock starts to occur causing lower efficiency in braking and the deceleration rate decreases.

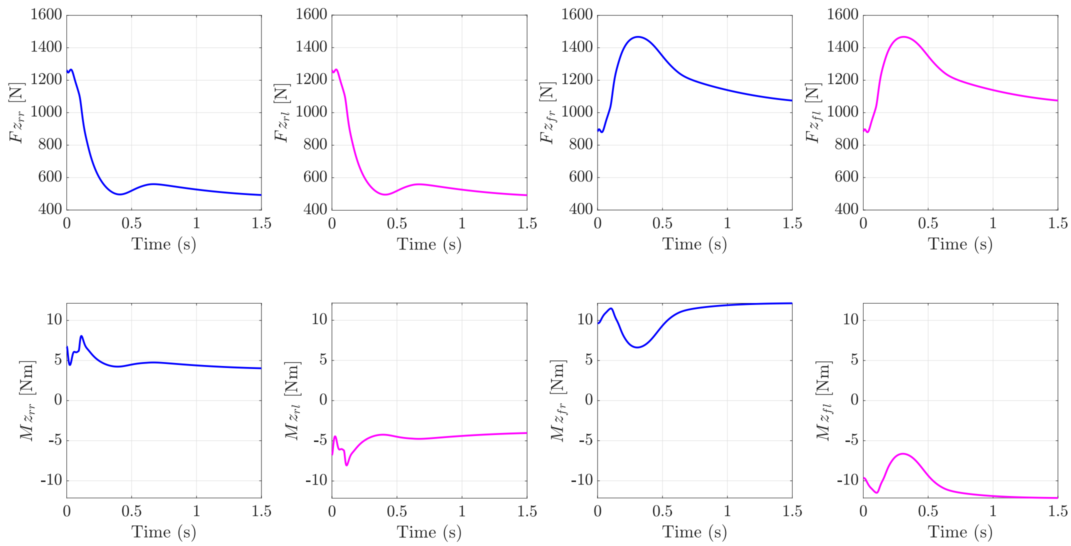

Figure 4.7: Vertical forces F_z and self aligning torque M_z [maneuver #2]

Figure 4.7 shows the vertical force F_z has decreased in the rear tires while increasing in the front. This is attributed to the longitudinal load transfer to the front because of the braking. The F_z forces on all tires showed a peak around 0.27 seconds due to the rear wheels locking.

No steering input means no side slip angle α for all tires [Figure 4.8]. And similar to maneuver #1, the right tires' lateral forces are opposite in direction compared to the left tires and equal in magnitude. The self aligning torque M_z profiles in Figure 4.7 for each tire are trying to counter the F_y's effect on the steering. F_y showed the same trend as F_z, increasing in the front while decreasing in the rear tires.

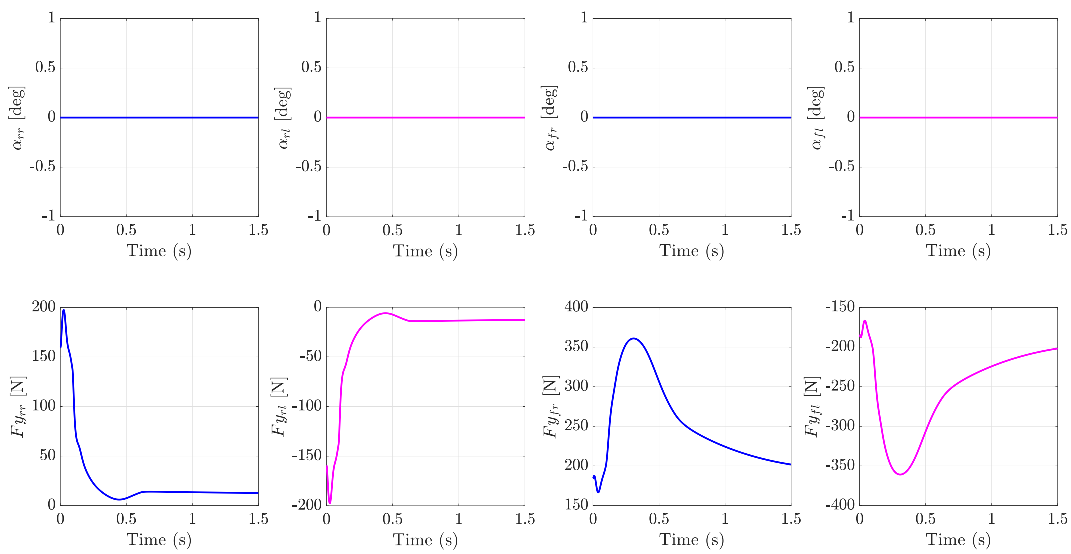

Figure 4.8: side slip angle α and lateral forces F_y [maneuver #2]

3. initial conditions: $u_0 = 50$ km/h
   simulation timing: $T_s = 0.001$ s, $T_f = 1.5$ s
   requested pedal: req_pedal = 0.5
   requested steering wheel angle: req_steer = 20 deg.

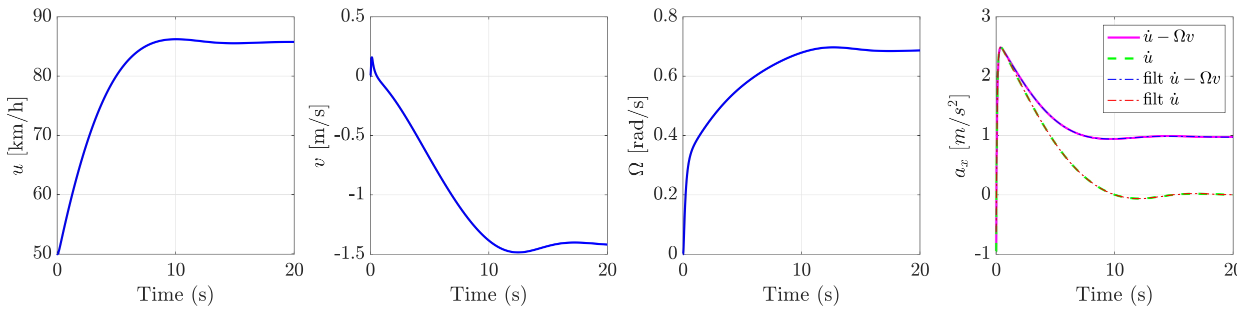

Figure 4.9: vehicle motion graphs [maneuver #3]

Figure 4.9 shows the motion graphs of the third maneuver. The longitudinal speed u keeps increasing until it reaches full saturation for half throttle. The lateral speed v shows the same profile as u. v is negative indicating the vehicle is turning left. The yaw rate Ω follows the same pattern, increasing during acceleration, and constant once acceleration is zero.

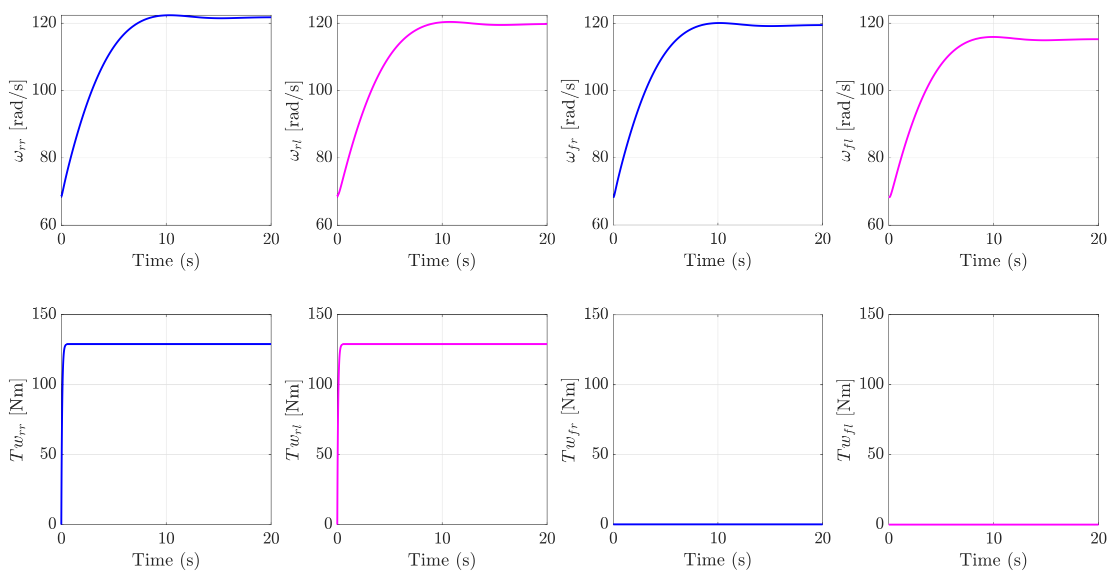

Figure 4.10: Wheel rates ω and Torques Tw [maneuver #3]

The angular velocity ω are different for different for each wheel as the outer [right] tires would need to rotate faster than the inner [left] tires [Figure 4.10]. The torque experienced by the rear tires are equal to each other, while the front ones are zero.

The longitudinal slip κ relies on ω for each wheel and can be calculated using Equation 4.2:

$$\kappa_{ij} = \frac{\omega_{ij} R_{ij} - \upsilon_{cxij}}{\upsilon_{cxij}} \quad i \in \{f, r\} \quad j \in \{r, l\} \tag{4.2}$$

Figure 4.11 shows κ and F_x. As there was no torque on the front tires, κ and F_x on the front tires were small. κ for the rear tires are different because they are rotating at different speeds. However, both rear tires still experienced the same F_x.

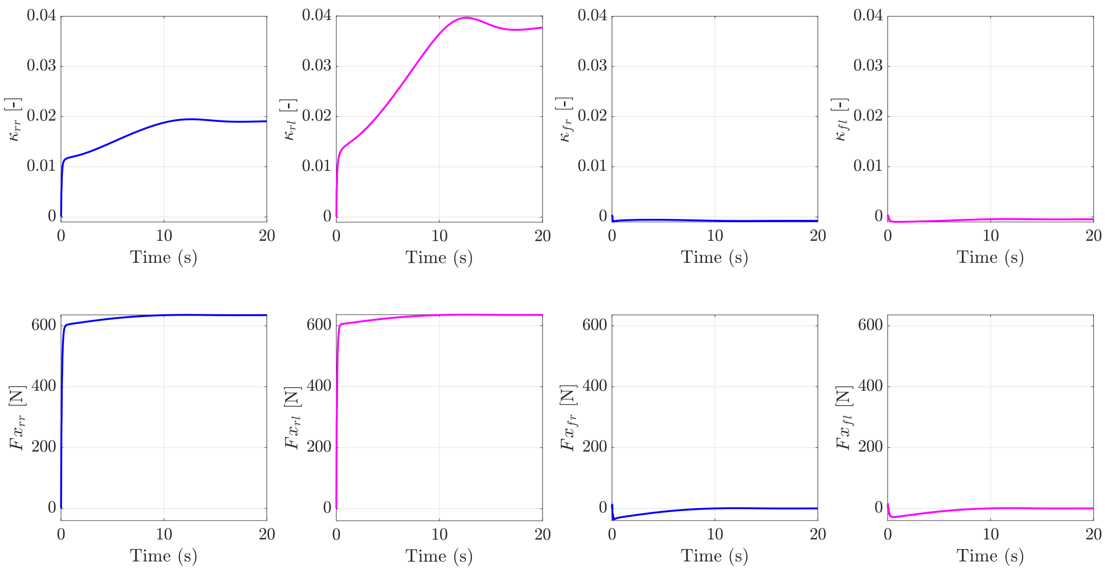

Figure 4.11: longitudinal slip κ and longitudinal forces F_x [maneuver #3]

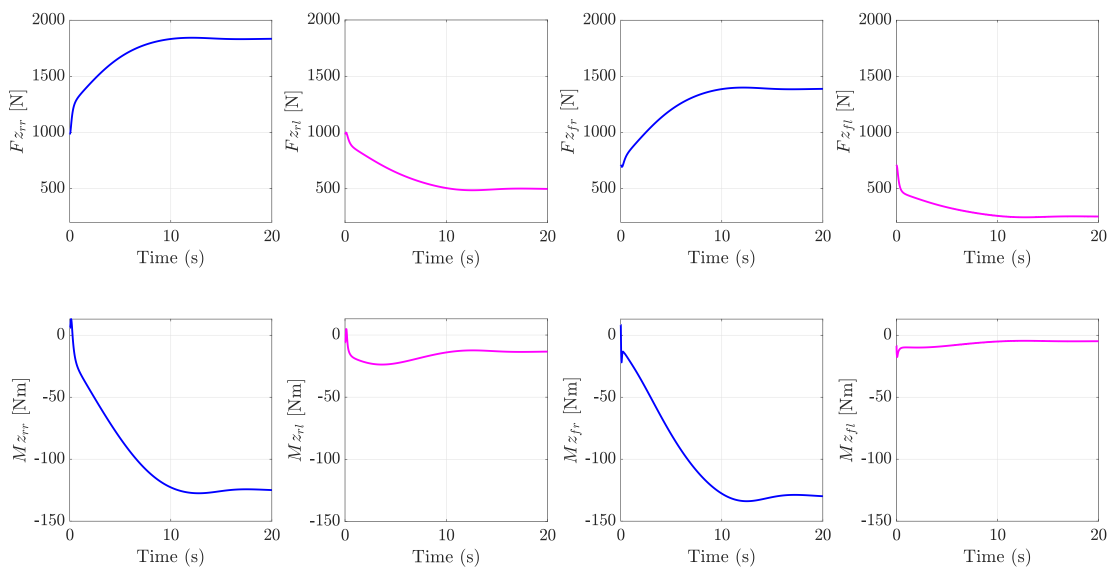

Figure 4.12: Vertical forces F_z and self aligning torque M_z [maneuver #3]

Figure 4.12 shows the vertical forces F_z for the right [outer] tires increasing then becoming constant when acceleration becomes zero. The left [inner] tires experienced the opposite because of the lateral load transfer to the right side of the vehicle due to the left turn.

The lateral side slip α for all tires are calculated using Equation 4.3:

$$\alpha_{ij} = -\arctan(\frac{vc_{yij}}{vc_{xij}}) \quad i \in \{f, r\} \quad j \in \{r, l\} \tag{4.3}$$

α appears to be consistent across the four tires as shown in Figure 4.13. However, the rear tires are slightly higher due to the torque applied by the motors.

The right side tires have higher lateral forces F_y compared to the right. This is because F_y relies on F_z, as the the lateral load transferred to the right side during the left turn maneuver. Both α and F_y become constant once the acceleration is equal to zero. The self aligning torque M_z profiles in Figure 4.12 for each tire are trying to counter the F_y's effect on the steering.

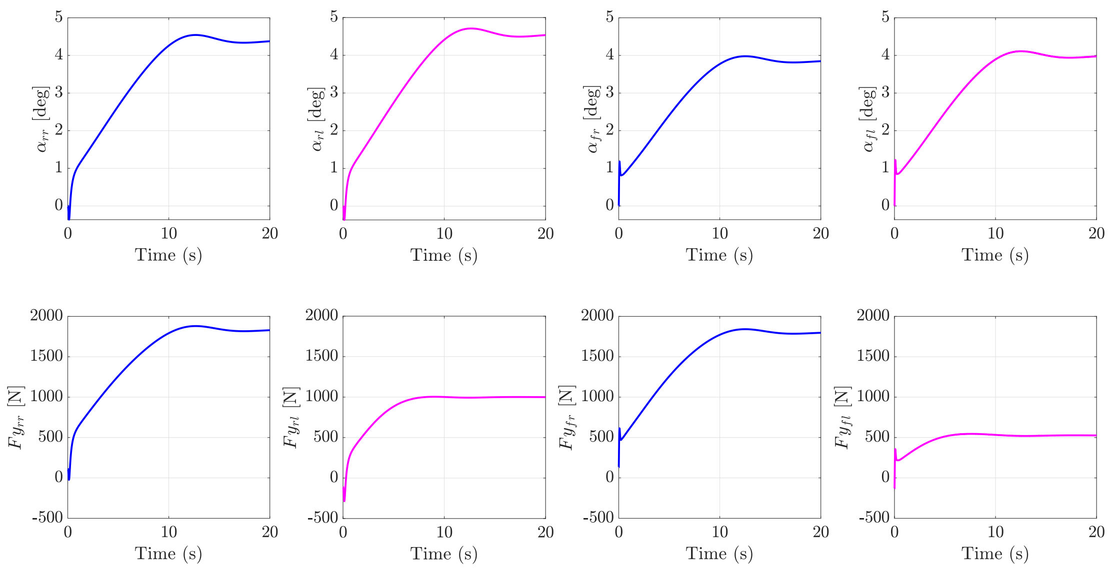

Figure 4.13: side slip angle α and lateral forces F_y [maneuver #3]

Assignment 5

Handling Identification

5.1 Exercise 1 - Sine Steer Maneuvers

Q. Perform a set of sine steer maneuvers, with steering wheel angle $\delta_D = \delta_{D0} \sin(2\pi f t)$. Use $\delta_{D0} = 5°$, and repeat the test at 3 different u = {50, 80, 100} km/h.

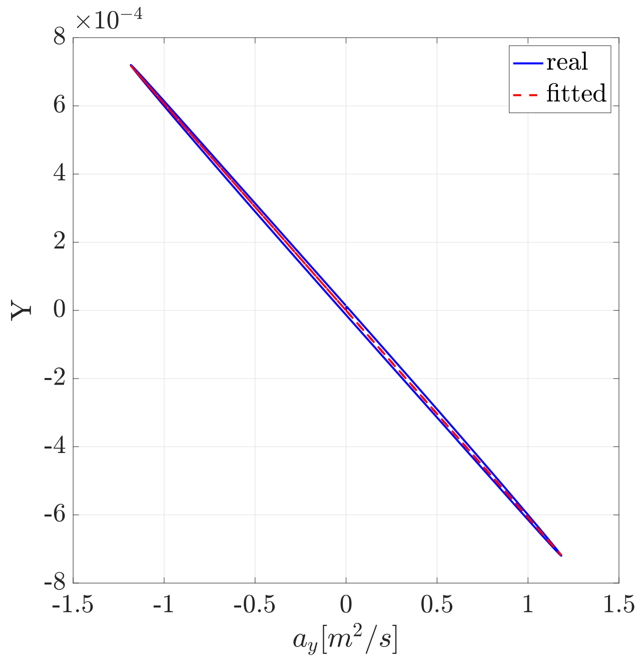

Figure 5.1: Fitted handling diagram result [$\delta_{D0} = 5°$, u = 50 km/h]

Figure 5.1 shows the handling diagram result of a sine steering maneuver that uses a desired steering angle $\delta_D = \delta_{D0} \sin(2\pi f t)$ at speed 50 km/h. The frequency f in the equation is the number of complete cycles that happen every second. We must perform changes to our system very slowly in order to preserve steady state conditions. The frequency used was 0.001 s^{-1} and the simulation time was 1000 seconds. The Y refers to the handling behaviour of the vehicle and is calculated using Equation 5.1:

$$Y = \delta - \frac{\Omega}{u}L \tag{5.1}$$

The handling curve obtained at 50 km/h has a negative slope and appears to be linear. The data can be fitted with a first degree polynomial [$f(x) = ax + b$] as shown in Figure 5.1.

The negative slope indicates that the vehicle exhibits an over-steering behaviour. Over-steering occurs when the vehicle's rear wheels have higher lateral slip compared to the front [$\alpha_r > \alpha_f$]. This causes the rear wheels to have a larger radius of curvature than the front and the vehicle steers more than expected. If we want to keep the same radius of curvature in an over-steering condition, we must decrease the steering angle δ at higher velocities.

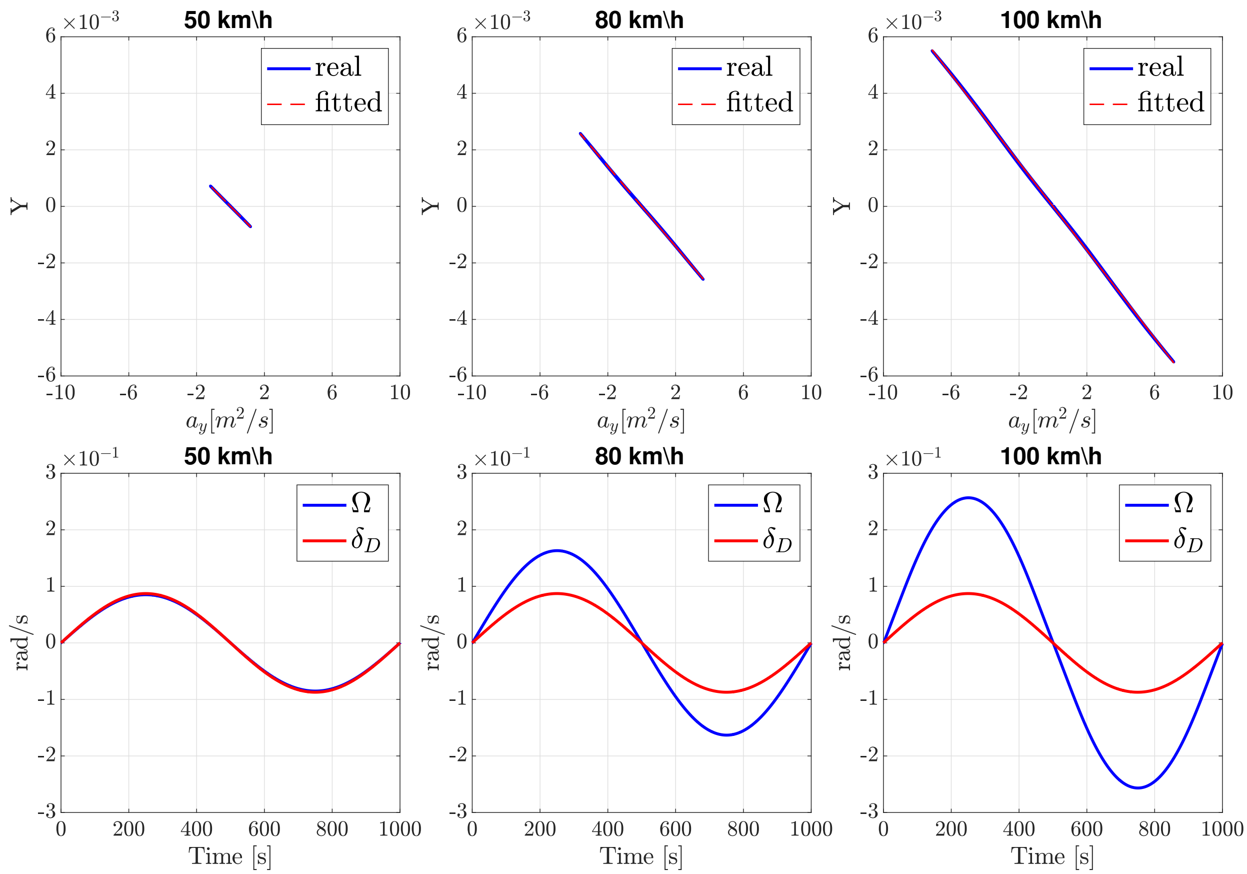

Figure 5.2: Handling diagram results at different speeds with same δ_D

The slope of the line represents the under-steering gradient K_{us}. It describes the evolution of δ as a_y increases. K_{us} is positive if the vehicle is under-steering and negative when over-steering.

Increasing the speeds to 80 and 100 km/h resulted in an increase in the lateral acceleration a_y as shown in Figure 5.2. The vehicle nonetheless showed over-steering behaviour across all the simulated speeds. A comparison between the yaw-rate Ω and the desired steering angle δ_D shows that the Ω keeps increasing with higher speeds while δ_D does not.

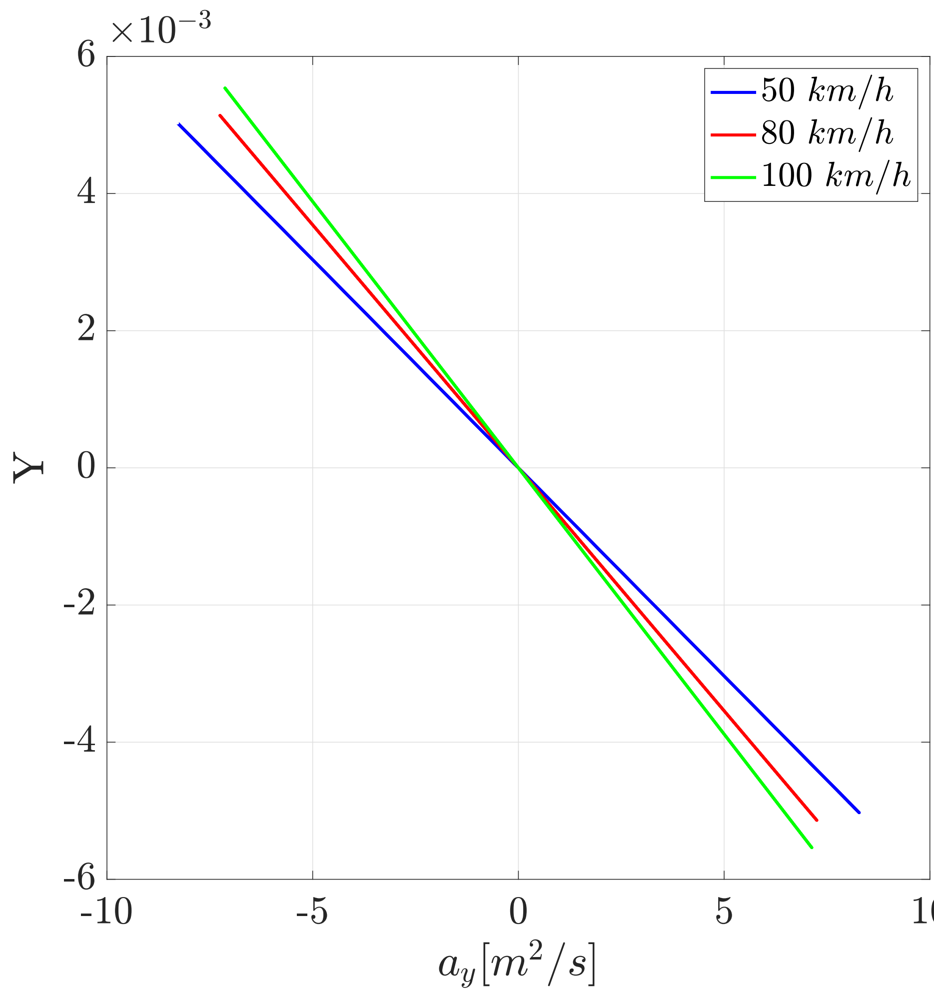

Figure 5.3: Fitted handling curves comparison with same δ_D

Superimposing the handling curves of the three simulated speeds in Figure 5.3 clearly shows that with higher speeds, the over-steering behavior increases [steeper negative slope]. That means δ will need to be decreased even further with higher speeds to keep the same curvature. Furthermore, the obtained curves pass through the origin. That means when there is no lateral acceleration a_y, the steering behaviour will be neutral.

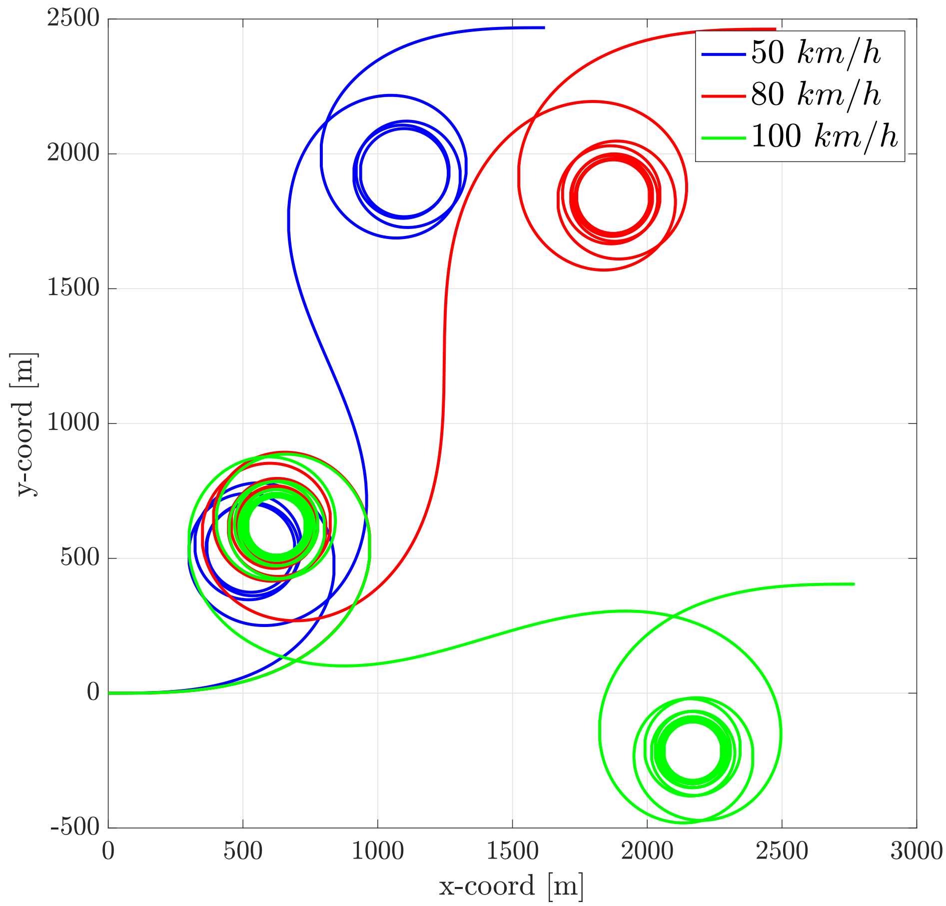

Figure 5.4: Vehicle paths for sine steer at different speeds with same δ_D

Plotting the path results of the three different speeds, as shown in Figure 5.4, confirms the over-steering behaviour. The radius of the curvature [the size of the circles] decreases with increasing velocities.

Q. carry out other 3 sine steer maneuvers, with these data:

1. $\boldsymbol{\delta_{D0} = 70°}$ **,** $\boldsymbol{u = 50}$ **km/h**
2. $\boldsymbol{\delta_{D0} = 24°}$ **,** $\boldsymbol{u = 80}$ **km/h**
3. $\boldsymbol{\delta_{D0} = 12°}$ **,** $\boldsymbol{u = 100}$ **km/h**

Figure 5.5 shows the results of maintaining the vehicle's longitudinal velocity u at 50 km/h. A sinusoidal steering maneuver was applied with a large amplitude [70°] and a frequency f of 0.001 s^{-1}. This maneuver shows that the vehicle's handling behaviour changes when the lateral acceleration a_y increases above a certain threshold.

The previous runs only had a maximum steering angle of 5°, which is considered small. With a much bigger maximum steering angle of 70°, the vehicle exhibits a linear over-steering behaviour while a_y is below 10 m^2/s. Once full saturation is reached, the slope of the curve becomes positive indicating that the behaviour has switched to under-steer.

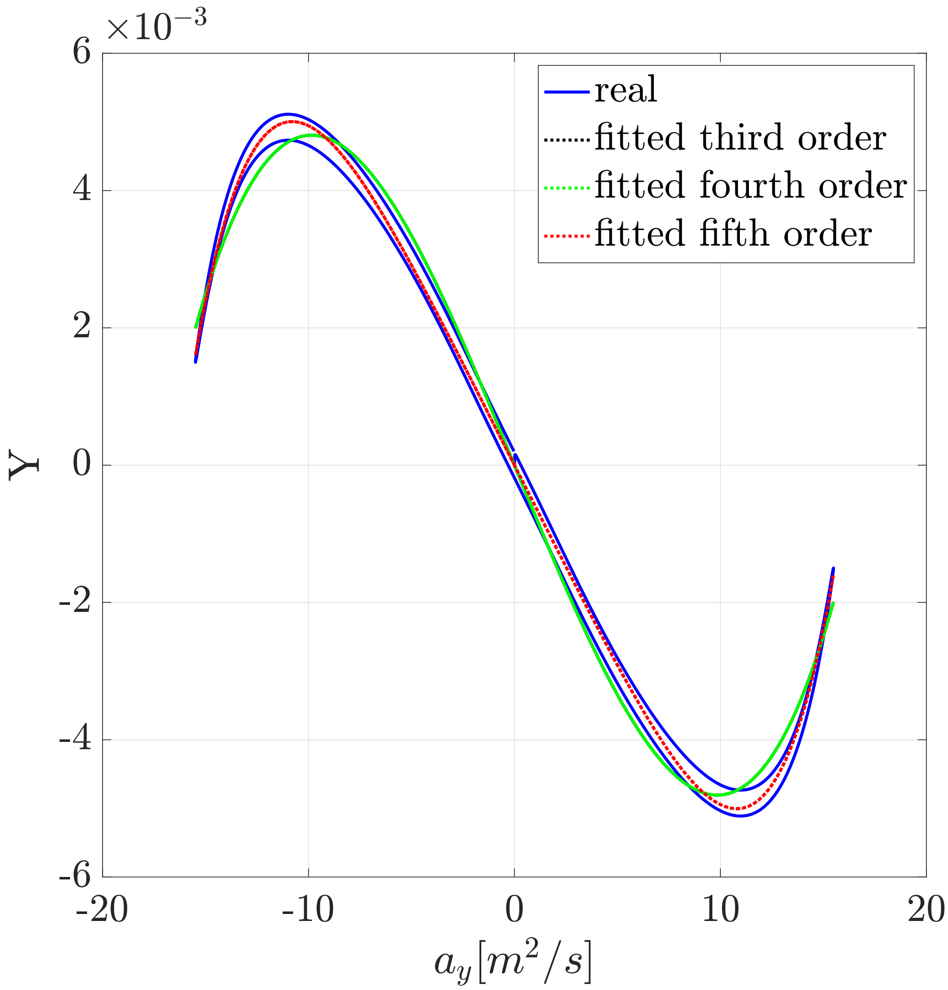

Figure 5.5: Fitted handling diagram result [δ_{D0} = 70°, u = 50 km/h]

The curve can no longer be fitted with a first degree polynomial. Polynomial degrees from one to five were tested, and the lowest and best fitting ones are shown in Figure 5.5. It appears that a fifth order polynomial is the best approximation for such a curve.

Figures 5.6 and 5.7 show the results of the second and third runs. The effect of higher lateral acceleration a_y on the handling behaviour is not as prevalent in both runs, because the maximum steering angle was much smaller [12° and 24° compared to 70°]. The overall behaviour for the second and third runs stayed as over-steering across a_y. However, the curve is not linear. A third order polynomial was the best fitting for both runs.

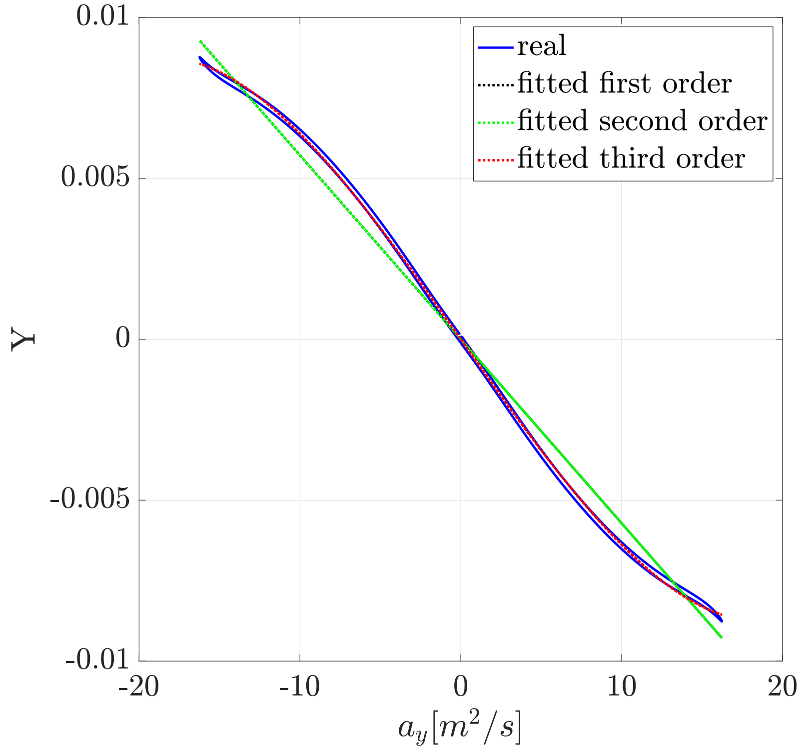

Figure 5.6: Fitted handling diagram result [δ_{D0} = 24°, u = 80 km/h]

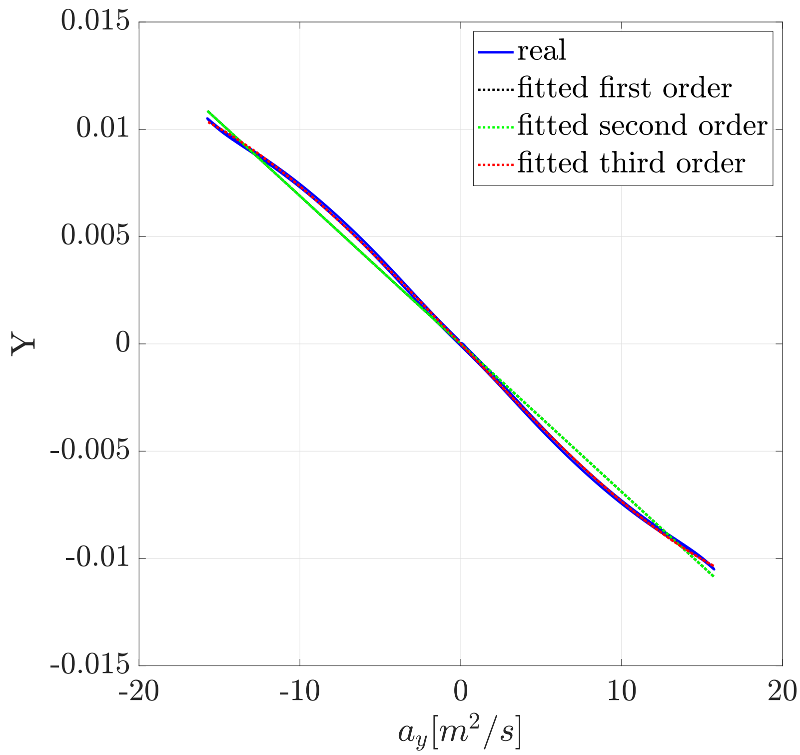

Figure 5.7: Fitted handling diagram result [δ_{D0} = 12°, u = 100 km/h]

Coefficients of the polynomial fittings:
run# 1: [0.0013296, -1.6137e-07, 0.0003224, 3.9837e-07, -0.0066391, -1.9657e-07]
run# 2: [0.0010692, 6.2659e-08, -0.0082143, -9.0719e-08]
run# 3: [0.0007569, 7.6441e-08, -0.0089127, -8.4754e-08]

The results of all the coefficients for the fittings for the three runs are shown above. They are certainly not constant across the runs because they fit different curves. However, some are quite close, especially runs # 2 and 3. This could be attributed to the similarity in the linear sections of the three curves as shown in Figure 5.8.

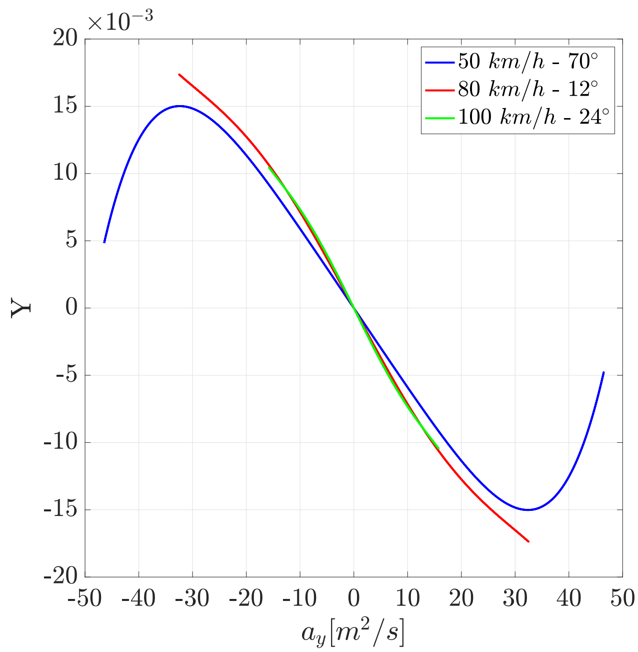

Figure 5.8: Fitted handling curves comparison with different δ_D

5.2 Exercise 2 - Constant Steer Maneuvers

Q. Carry out a constant steering maneuver, with these data:

1. $\boldsymbol{\delta_D = 10°}$ **,** $\boldsymbol{u_0 = 20}$ **km/h ,** $\boldsymbol{u_f = 40}$ **km/h**
2. $\boldsymbol{\delta_D = 24°}$ **,** $\boldsymbol{u_0 = 50}$ **km/h ,** $\boldsymbol{u_f = 80}$ **km/h**

The simulations were run for 1000 seconds. Figure 5.9 shows the motion graphs for maneuver #1 [only plotting the first 10 seconds]. The speed ramped up from 20 to 40 km/h within the first 2 seconds using the low level PID controller to manage the pedal.

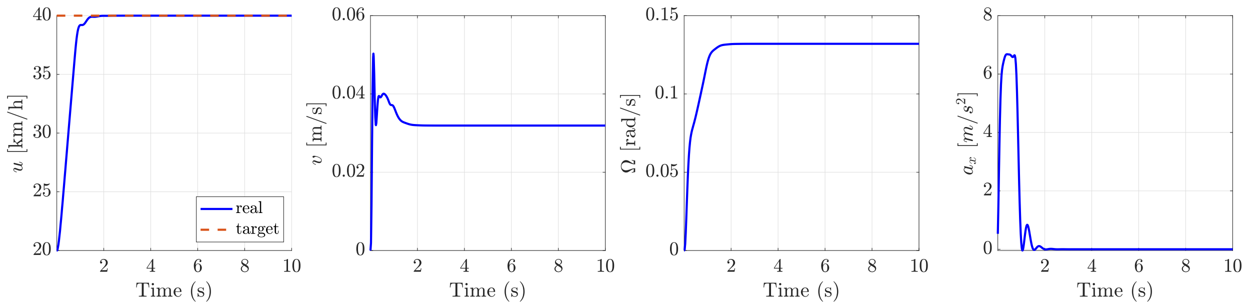

Figure 5.9: Vehicle motion graphs for constant steer maneuver #1

The vehicle must be in steady state conditions in order to plot the handling curve. The data was filtered by monitoring the change in u using Equation 5.2. The data used in plotting begins at the (steady state start index) till the end [Figure 5.10].

$$\text{steady state start index} = \text{find (diff (} u \text{)) } >= 0.003 m/s \tag{5.2}$$

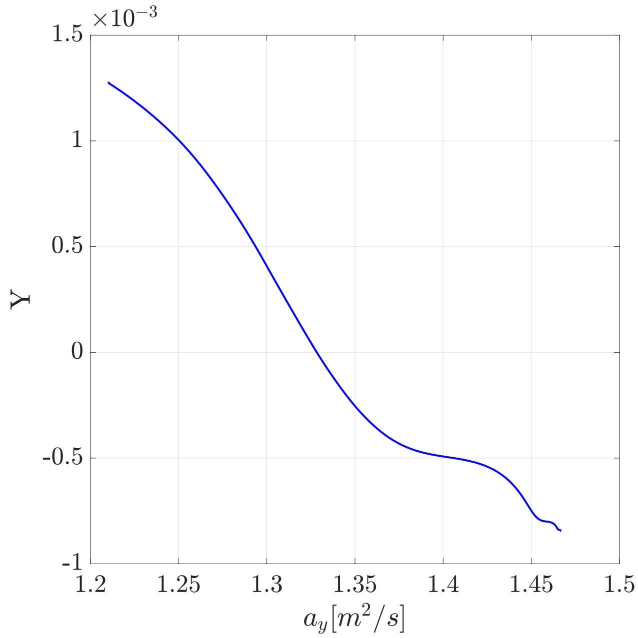

Figure 5.10: Filtered handling curve for constant steer maneuver #1

Even though the filtering has significantly improved the result of the graph, it still is not quite accurate enough. This might be due to the very low lateral acceleration a_y that the vehicle experienced during this maneuver. Nonetheless, the results still suggests that the vehicle has an over-steering behaviour.

The path result of the maneuver plotted in Figure 5.11 shows that the curve was about 80 meters in radius and the vehicle ended almost at the start point. This indicates that the vehicle experienced a negligible amount of over-steer as it was not pushed hard enough to cause any front or rear tire slip.

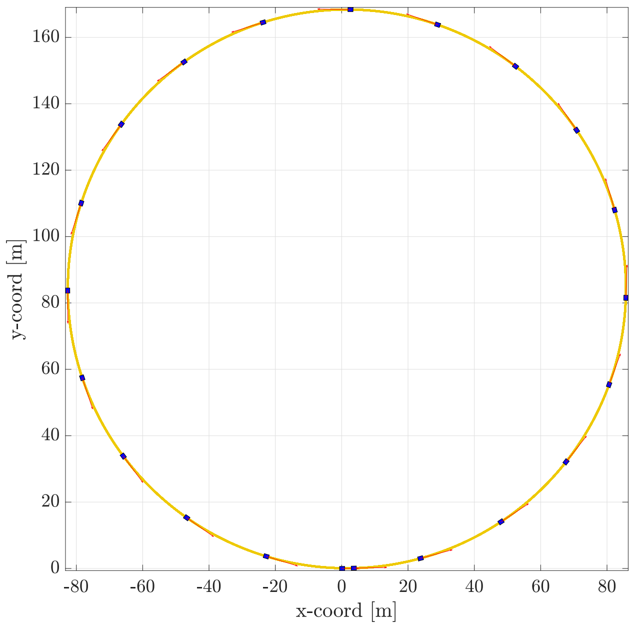

Figure 5.11: Path of the vehicle for constant steer maneuver #1

Similar to maneuver #1, Figure 5.12 shows the motion graphs for maneuver #2 [only plotting the first 10 seconds]. The speed ramped up from 40 to 80 km/h within the first 3 seconds using the low level PID controller to manage the pedal.

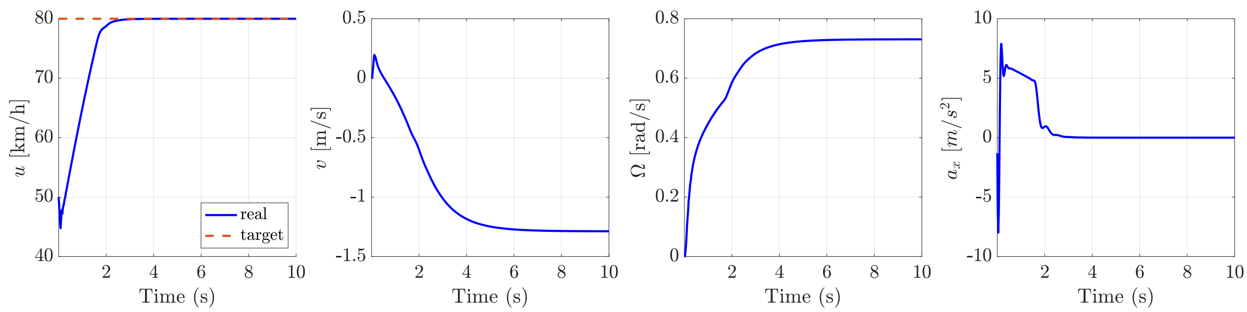

Figure 5.12: Vehicle motion graphs for constant steer maneuver #2

The filtered handling curve for maneuver #2 in Figure 5.13 is significantly better than the previous maneuver. this could be attributed to the much higher lateral acceleration a_y encountered. The curve is almost linear and has a negative slope, which agrees with all the previous maneuvers.

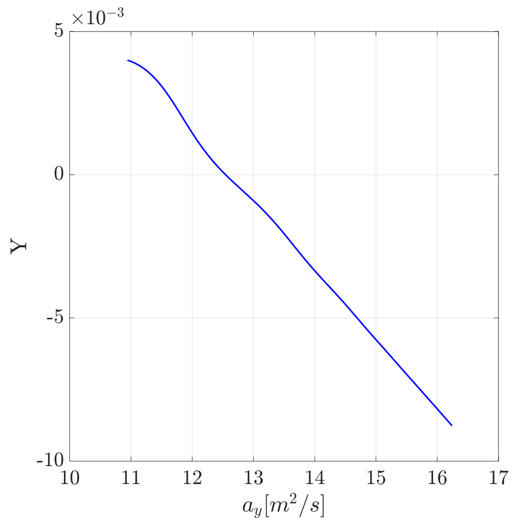

Figure 5.13: Filtered handling curve for constant steer maneuver #2

The radius of the path with the second maneuver plotted in Figure 5.14 has a much smaller radius [40 meters]. The vehicle has certainly experienced over-steer because the curvature decreased towards the end of the run.

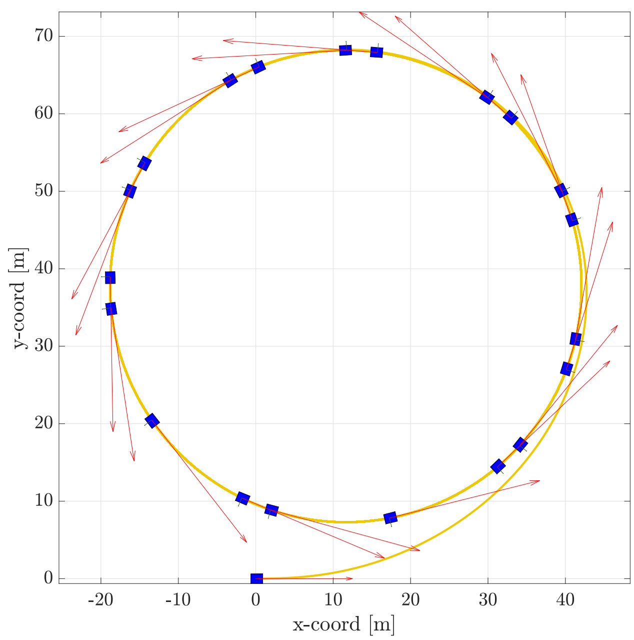

Figure 5.14: Path of the vehicle for constant steer maneuver #2

In conclusion, the steering gradient K_{us} is a function of multiple variables including (a_y, u, a_x). To predict handling behaviour more accurately, the vehicle was tested from 20 to 100 km/h using the sine steer maneuver with a $\delta_D = 10°$. The results are in Table 6.1 and Figure 5.15.

u **[km/h]**	K_{us}
20	-1.0×10^{-4}
30	-3.0×10^{-4}
40	-6.0×10^{-4}
50	-1.0×10^{-3}
60	-1.6×10^{-3}
70	-2.4×10^{-3}
80	-3.5×10^{-3}
90	-5.0×10^{-3}
100	-6.9×10^{-3}

Table 5.1: Vehicle's K_{us} for tested speeds with sine steer [$\delta_D = 10°$]

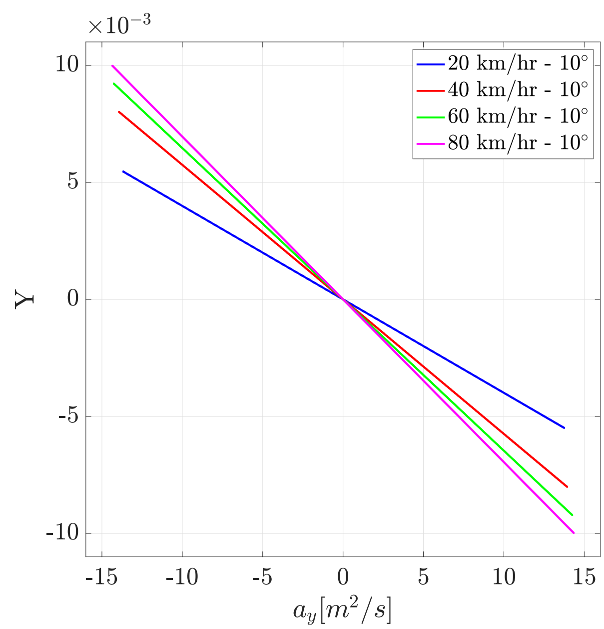

Figure 5.15: K_{us} results based on u with sine steer [$\delta_D = 10°$]

Sine steer	**Constant Steer**
More difficult to maintain steady state as the steering angle is changing constantly	Easier to maintain steady state considering that u is easier to regulate
Needs a robot to perform	Easily performed by a human driver
Perform left and right turns on the same run	Only perform either left or right turns per run
Requires a larger area to perform [going straight and steering left to right]	A smaller area is required to perform [going in circles]

Table 5.2: Pros And Cons of the constant steer and sine steer tests

Assignment 6

Lateral Control

6.1 Exercise 1 - lateral control

Q. Optimize the clothoid-based lateral controller

The clothoid-based lateral controller uses Equation 6.1 to calculate the steering angle required to follow the clothid. The under-steering gradient K_{us} was calculated previously using the handling diagram and the results were shown in Table 6.1 and Figure 6.1. These results were implemented as a variable that changes based on the vehicle's current speed.

$$\delta(s) = k(s)(L + K_{us}u^2) \tag{6.1}$$

To optimize the clothoid-based lateral controller look ahead variable, several tests were conducted using the following variables totalling 42 tests in total:

- u = [10, 20, 30, 40, 50, 60, 70, 80] km/h
- look ahead = [5, 10, 15, 20, 25, 30]

The tracking error had to be calculated to compare the tests' results. That was done by using the "N-D nearest point search" function in Matlab, which returns indices of closest points in the desired path for each point on the real path. Then calculating the euclidean distance between each point in the real path and closest point on the desired path as tracking error. The results are shown in Figure 6.1 and Table 6.1.

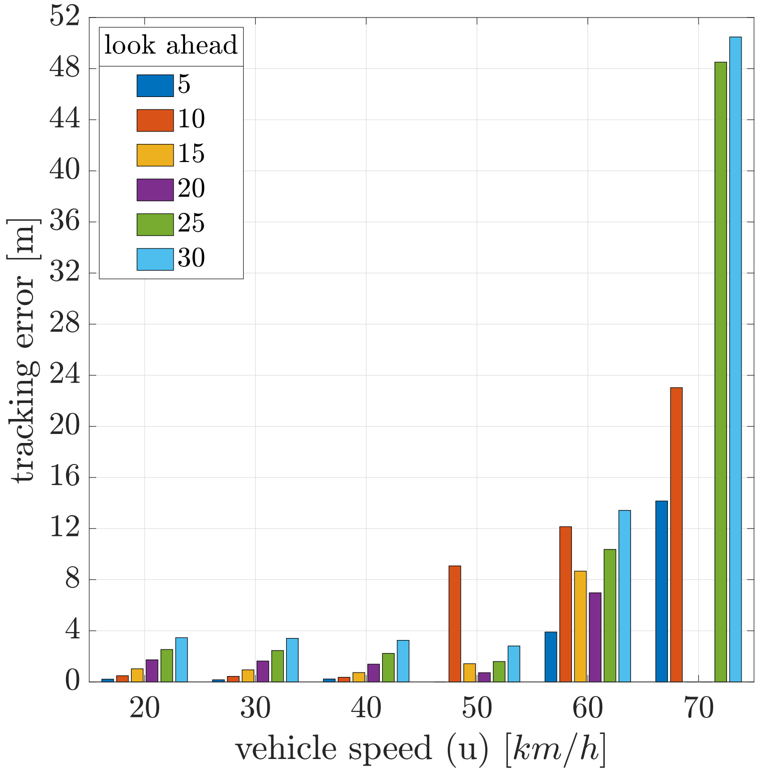

Figure 6.1: clothoid-based lateral controller at different u and look ahead

The tests checked if the vehicle was able to arrive at a designated target point chosen to be at [60,10]. If the vehicle reaches this point within a threshold of 5 meters, the test is considered a success.

u **[km/h]**	**LA = 5**	**LA = 10**	**LA = 15**	**LA = 20**	**LA = 25**	**LA = 30**
20	2.1×10^{-1}	4.8×10^{-1}	1.0	1.7	2.5	3.5
30	1.6×10^{-1}	4.3×10^{-1}	9.4×10^{-1}	1.6	2.5	3.4
40	2.3×10^{-1}	3.6×10^{-1}	7.3×10^{-1}	1.4	2.2	3.3
50	NA	9.1	1.4	7.2×10^{-1}	1.6	2.8
60	NA	1.2×10^{1}	8.7	7.0	1.0×10^{1}	1.3×10^{1}
70	1.4×10^{1}	2.3×10^{1}	NA	NA	4.9×10^{1}	5.0×10^{1}

Table 6.1: Tracking error results [clothoid-based lateral controller]

The red colored cells indicates the vehicle was not able to arrive at the designated target point. Green cells are the chosen look ahead values at each speed u.

It appears that the larger the look ahead value, the larger the tracking error as expected. Having a larger look ahead at 20 km/h could be beneficial if we are optimizing for traveled distance, and smoother turns [less jerk].

Figure 6.2 shows the vehicle actual path at each look ahead value for 20 km/h tests. A larger look ahead optimized the vehicles path to take a shorter route and take better turns. However, this caused the tracking error to increase, because we are not following the reference trajectory anymore.

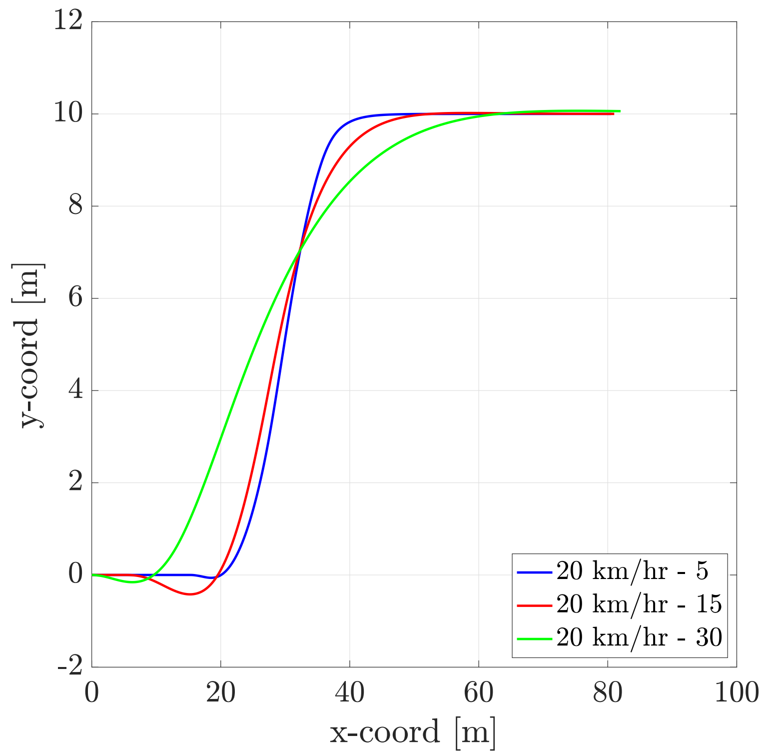

Figure 6.2: Real vehicle path with different look ahead values [u = 20km/h]

Up until 40 km/h, a lower look ahead value performed better for our metrics. With increasing u, the smaller look ahead values were simply not enough to control the vehicle properly. The controller needs to see far enough ahead to account for a curve earlier on. The faster the vehicle, the bigger the needed look ahead value. However, it seems that after 70 km/h, the vehicle can no longer become stable even with a look ahead as high as 250.

Figure 6.3 shows the vehicle paths at 70 km/h at different values for the look ahead. The higher values are more stable but still considered outside the capabilities of the vehicle.

No values of look ahead was enough to stabilize the vehicle with any speed higher than 70 km/h. This might be attributed to the K_{us} values not accurate enough at these speeds. The handling curves during these speeds were not linear anymore and a linear approximation for them is not sufficient.

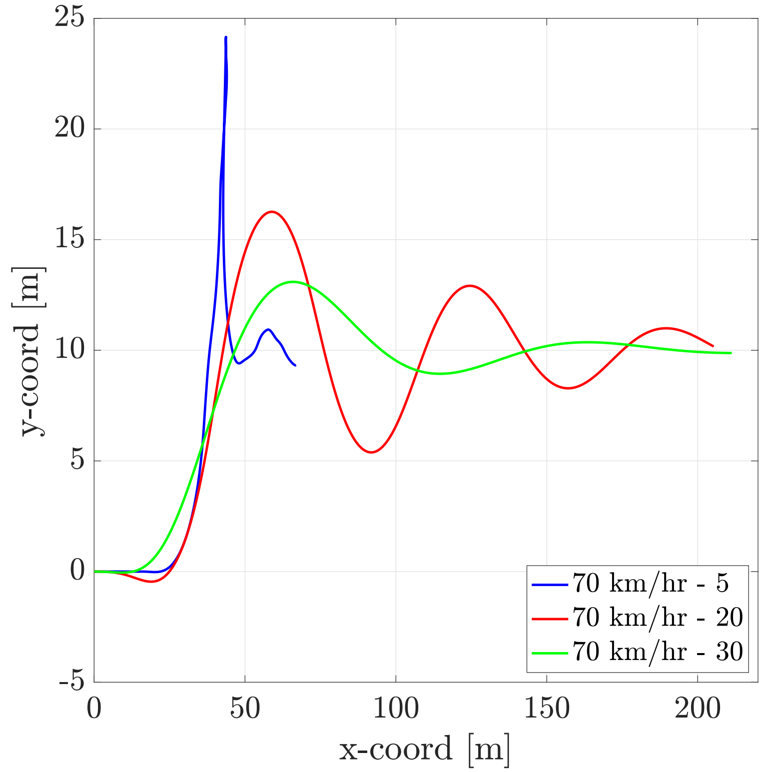

Figure 6.3: Real vehicle path with different look ahead values[u = 70km/h]

Q. Implement the pure pursuit controller and optimize the look ahead distance